



저작자표시-비영리-변경금지 2.0 대한민국

이용자는 아래의 조건을 따르는 경우에 한하여 자유롭게

- 이 저작물을 복제, 배포, 전송, 전시, 공연 및 방송할 수 있습니다.

다음과 같은 조건을 따라야 합니다:



저작자표시. 귀하는 원저작자를 표시하여야 합니다.



비영리. 귀하는 이 저작물을 영리 목적으로 이용할 수 없습니다.



변경금지. 귀하는 이 저작물을 개작, 변형 또는 가공할 수 없습니다.

- 귀하는, 이 저작물의 재이용이나 배포의 경우, 이 저작물에 적용된 이용허락조건을 명확하게 나타내어야 합니다.
- 저작권자로부터 별도의 허가를 받으면 이러한 조건들은 적용되지 않습니다.

저작권법에 따른 이용자의 권리는 위의 내용에 의하여 영향을 받지 않습니다.

이것은 [이용허락규약\(Legal Code\)](#)을 이해하기 쉽게 요약한 것입니다.

[Disclaimer](#)

Comparison of GALC gene editing  
efficiency between ABE8e and  
ABE8eWQ in a mouse model of Krabbe's  
disease

*Joo-Hee Kim*

Department of Medical Science

The Graduate School, Yonsei University

Comparison of GALC gene editing  
efficiency between ABE8e and  
ABE8eWQ in a mouse model of Krabbe's  
disease

Directed by Professor Sung-Rae Cho

The Master's Thesis  
submitted to the Department of Medical Science,  
the Graduate School of Yonsei University  
in partial fulfillment of the requirements for the degree of  
Master of Medical Science

Joo-Hee Kim

June 2023

This certifies that the Master's Thesis of  
Joo-Hee Kim is approved.

---

Thesis Supervisor : Sung-Rae Cho

---

Thesis Committee Member#1 : Hyongbum Henry Kim

---

Thesis Committee Member#2 : Sangsu Bae

The Graduate School  
Yonsei University

June 2023

## ACKNOWLEDGEMENTS

My greatest debt is to professor Sung-Rae Cho, who has guided me, supervised me and motivated me to continue this research work. I would also like to thank professor Hyung-bum Kim and Sang-su Bae who advised on the research and supplementary directions as thesis committee members. Their practical advice and academic support were incredibly helpful.

Thanks to my colleagues and participating investigators, I was able to freely discuss the direction of the study and keep working to complete this dissertation. Lastly, I appreciate my supportive friends and all the members of my extended family including my parents. Without their encouragement and infinite love, I couldn't have dared to complete all my tasks.

## <TABLE OF CONTENTS>

ABSTRACT .....	vi
I. INTRODUCTION .....	1
II. MATERIALS AND METHODS .....	3
1. Vector design and production .....	3
2. Animals and animal welfare .....	4
3. Neonatal stereotaxic surgery on postnatal day 1 .....	4
4. Behavior assessments .....	6
5. Mouse sacrifice .....	7
6. RNA isolation .....	7
7. Quantitative real-time-polymerase chain reaction (qRT-PCR) .....	8
8. High-throughput sequencing .....	8
9. Immunofluorescence (IF) .....	8
10. Hematoxylin and eosin staining .....	9
11. Luxol fast blue/ Periodic acid schiff staining .....	9
12. Transmission electron microscopy (TEM) .....	9
13. DTI metric acquisition and comparison .....	10
14. Statistical analysis .....	10
III. RESULTS .....	12
1. mRNA expression of split ABEs was significantly higher in frontal cortex and corpus callosum .....	12
2. Adenine editing accuracy of ABE8eWQ was higher than that of ABE8e .....	15
3. Both ABE8e and ABE8eWQ preserved weight loss of twitcher mice ·	22
4. Both ABE8e and ABE8eWQ ameliorated neurobehavioral impairments of twitcher mice .....	25

5. Both ABE8e and ABE8eWQ increased the lifespan of twitcher mice	· 33
6. Both ABE8e and ABE8eWQ increased the expression of myelin basic protein in corpus callosum of twitcher mice	· 35
7. Both ABE8e and ABE8eWQ restored myelination in the corpus callosum, but not myelination in the sciatic nerve	· 39
8. Both ABE8e and ABE8eWQ increased myelin integrity and decreased the number of PAS-positive cells	· 44
9. Both ABE8e and ABE8eWQ induced white matter recovery in the diffusion tensor images of brain MRI	· 47
10. Low mRNA expression of split ABEs and gene editing efficiency were shown in heart, liver, spinal cord and sciatic nerve	· 52
11. Tumor or dysplasia was not identified in brain, heart, liver and spinal cord after ABE treatments	· 59
12. ABE treatments to wild-type mice produced no statistical difference in all behavioral assessments	· 61
13. ABE treated wild-type mice showed no behavioral abnormalities despite aging corpus callosum	· 67
14. Few RNA off-target effects were found after ABE treatments	· 70
 IV. DISCUSSION	· 72
V. CONCLUSION	· 74
 REFERENCES	· 75
ABSTRACT(IN KOREAN)	· 78
PUBLICATION LIST	· 79

## LIST OF FIGURES

Figure 1. Injection materials encoding adenine base editor (ABE) ..	3
Figure 2. The experimental scheme for animal model .....	5
Figure 3. Genotype for twitcher identification .....	6
Figure 4. Behavioral assessment .....	7
Figure 5. RNA expression levels of viral vectors in four specific brain regions .....	12
Figure 6. Gene editing window of ABE8e and ABE8eWQ .....	15
Figure 7. Gene editing efficiency of ABE8e and ABE8eWQ in four brain regions .....	16
Figure 8. Body weights and brain weights in twitcher groups .....	22
Figure 9. Clasping test in twitcher groups .....	26
Figure 10. Rotarod scores in twitcher groups (4 rpm) .....	27
Figure 11. Rotarod scores in twitcher groups (12 rpm) .....	28
Figure 12. Rotarod scores in twitcher groups (4-12 rpm) .....	29
Figure 13. Lifespan and survival rate .....	34
Figure 14. Immunohistochemical expression of myelin basic protein (MBP) .....	36
Figure 15. Transmission electron microscopy (TEM) images of corpus callosum .....	40
Figure 16. Transmission electron microscopy (TEM) images of sciatic nerve .....	41
Figure 17. LFB/PAS staining analysis on remyelination following	

ABE treatment .....	44
Figure 18. Diffusion tensor imaging (DTI) analysis of the brain ..	48
Figure 19. RNA expression levels of viral vectors in heart, liver, spinal cord and sciatic nerve .....	52
Figure 20. Gene editing efficiency of ABE8e and ABE8eWQ in heart, liver, spinal cord and sciatic nerve .....	55
Figure 21. Hematoxylin and eosin staining of six brain regions ....	59
Figure 22. Hematoxylin and eosin staining of heart, liver and spinal cord .....	60
Figure 23. Body weights in ABE treated wild-type mouse groups ..	61
Figure 24. Clasp test in ABE treated wild-type mouse groups ..	62
Figure 25. Rotarod scores in ABE treated wild-type mouse groups .....	60
Figure 26. Behavioral assessments in ABE-treated wild-type old mice .....	67
Figure 27. Off-target RNA base editing in frontal cortex, corpus callosum, heart and liver .....	70

## LIST OF TABLES

Table 1. Heterogeneity of variance information of mRNA expression in the four specific brain regions .....	13
Table 2. Statistical information of mRNA expression in the four specific brain regions .....	13
Table 3. Heterogeneity of variance information of gene editing efficiency of target adenine (A5) .....	16
Table 4. Heterogeneity of variance information of gene editing efficiency of bystander adenine (A7) .....	17
Table 5. Heterogeneity of variance information of gene editing efficiency of bystander adenine (A10) .....	17
Table 6. Statistical information of gene editing efficiency of target adenine (A5) .....	18
Table 7. Statistical information of gene editing efficiency of bystander adenine (A7) .....	19
Table 8. Statistical information of gene editing efficiency of bystander adenine (A10) .....	20
Table 9. Heterogeneity of variance information of body weight and brain weight .....	23
Table 10. Statistical information of body weight and brain weight .....	24
Table 11. Heterogeneity of variance information of the behavioral assessment in twitcher mice .....	30

Table 12. Statistical information of the behavioral assessment in twitcher mice .....	31
Table 13. Heterogeneity of variance information of myelin basic protein expression .....	37
Table 14. Statistical information of myelin basic protein expression .....	38
Table 15. Heterogeneity of variance information of TEM image analysis .....	42
Table 16. Statistical information of TEM image analysis .....	43
Table 17. Heterogeneity of variance information of the number of PAS positive cells .....	45
Table 18. Statistical information of the number of PAS positive cells .....	46
Table 19. Heterogeneity of variance information of DTI parameters in the corpus callosum .....	49
Table 20. Heterogeneity of variance information of DTI parameters in the corpus callosum .....	50
Table 21. Heterogeneity of variance information of mRNA expression in heart, liver, spinal cord and sciatic nerve .....	53
Table 22. Statistical information of mRNA expression in heart, liver, spinal cord and sciatic nerve .....	54
Table 23. Heterogeneity of variance information of mRNA expression in heart, liver, spinal cord and sciatic nerven .....	56
Table 24. Statistical information of mRNA expression in heart, liver,	

spinal cord and sciatic nerve .....	57
Table 25. Heterogeneity of variance information of the behavioral assessment in wild-type mice .....	64
Table 26. Statistical information of the behavioral assessment in wild-type mice .....	65
Table 27. Heterogeneity of variance information of the behavioral assessment in old wild-type mice .....	68
Table 28. Statistical information of the behavioral assessment in old wild-type mice .....	69

## ABSTRACT

**Comparison of GALC gene editing efficiency  
between ABE8e and ABE8eWQ in a mouse model of Krabbe's disease**

Joo-Hee Kim

*Department of Medical Science  
The Graduate School, Yonsei University*

(Directed by Professor Sung-Rae Cho)

Krabbe disease is an autosomal recessive disease caused by the lack of GALC enzyme, which is required to hydrolyze certain toxic galactolipids. This leukodystrophy affects both the central nervous system and the peripheral nervous system. So far, therapeutic agents have been developed to treat Krabbe disease by injecting normal GALC gene. But we treated this disease by removing the genetic cause *in vivo* using adenine base editing (ABE).

In this study, using two types of adenine base editor, ABE8e and ABE8eWQ, we analyze not only their gene editing efficiency of target adenine, but also level of non-specific genetic alteration because these traits were directly related to the biological safety. ABE8eWQ was developed based on ABE8e to create a target-specific gene editor with increased editing efficiency of target adenine and reduced off-target effects. Therefore, experiment was conducted to confirm that ABE8eWQ has fewer side effects *in vivo*.

Gene editing efficiency of bystanders which are non-target adenines was significantly lower in ABE8eWQ compared to ABE8e. ABE-injected disease group, however, whether it was ABE8e or ABE8eWQ, demonstrated increased body and brain weight, higher behavioral test scores, decreased tremor and increased lifespan. Histological analysis of their brain also revealed better appearing myelin. Our study shows that both of ABEs, with no difference in side effects, helped alleviate overall disease symptoms of Krabbe disease.

---

Key words : krabbe disease, neurodegenerative disease, gene editing, adenine base editor, adeno-associated virus, demyelination

**Comparison of GALC gene editing efficiency  
between ABE8e and ABE8eWQ in a mouse model of Krabbe's disease**

Joo-Hee Kim

*Department of Medical Science  
The Graduate School, Yonsei University*

(Directed by Professor Sung-Rae Cho)

## I. INTRODUCTION

Krabbe disease (KD) is an autosomal recessive neurodegenerative disease caused by G (guanine) to A (adenine) point mutation in the gene encoding galactosylceramidase (GALC), which drives profound demyelination in whole nervous system.<sup>1</sup> Since GALC catabolized glycolipids including toxic compound named psychosine, deficiency of GALC results in accumulation of toxic substrates in myelin-related cells revoking myelin degradation, neuroinflammation and axonal degeneration.<sup>2,3</sup> Phenotypes of twitcher and wild-type mouse are similar before P21, but differ thereafter. Main symptoms of Krabbe disease including not only tremor but also weight loss, muscle weakness, hunchback and hindlimb paralysis appear around P21.

To date, many kinds of therapeutical approach have been studied including hematopoietic stem cell transplantation (HSCT), bone marrow transplantation (BMT) and AAV gene therapy of which purpose is to deliver GALC gene.<sup>4,5</sup> However, these treatments have a critical limitation that they do not eliminate the root cause of Krabbe disease, which is a G to A point mutation. In this study, we attempt to directly correct the mutated adenine using two types of adenine base editor, called ABE8e and ABE8eWQ.

Adenine base editing (ABE), a new-generation of gene editing technic, induce precise base change specially on adenine without double-stranded DNA breaks (DSB) and

homology-directed repair (HDR) on which one of the past-generation of gene editing technic, CRISPER genome editing, depends.<sup>6</sup> Single-nucleotide substitution occurs at upstream 12 to 17 nucleotide positions of protospacer adjacent motif sequence.<sup>7-10</sup> These characteristics suggested that ABE-mediated gene correction can be an effective gene therapy method to Krabbe disease.<sup>11,12</sup> To deliver ABEs, adeno-associated virus 9 (AAV9) were used as viral vectors which has ability to infect cells in vivo. Previous studies have been discovered that spliced ABE genes packaged in two AAV9 vectors expressed well in a mouse model of duchenne muscular dystrophy and tyrosinaemia, showing the high base editing efficiency.<sup>9,10</sup>

ABE8eWQ was created by developing ABE8e. We expected it can be a more precise and effective adenine base editor through minimizing undesired editing on non-target adenine. To verify this hypothesis, the editing efficiency of bystander adenine and the level of off-target effect were measured. Bystander adenine refers to non-target adenine within the editing window of ABE, and off-target effect refers to a phenomenon in which ABE operates in a completely wrong genetic location, increasing the potential risk due to undesired mutation. The reason why the off-target effect occurs is that ABE which does not properly attach to its target editing window may attach to a different place which has a sequence similar to its target editing window.

In conclusion, this study attempted to address the underlying cause of the Krabbe disease using adenine base editing. We did not simply use an adenine base editing to cure disease but conducted additional experiments and analysis on miscorrection of ABE8e and ABE8eWQ caused by non-specific binding.

## II. MATERIALS AND METHODS

### 1. Vector design and production

ABE8e and ABE8eWQ genes were respectively contained the guide RNA and the CMV promoter in two spliced AAV9 vectors. To conduct the stereotaxic surgery on P1 mouse model, pAAV200206-YP030 and pAAV200206-YP031 (VectorBuilder, Chicago, IL, USA) were used to AAV9 ABE8eWQ - NT ( $7.44 \times 10^9$  vg/ml), AAV9 ABE8eWQ - CT ( $1.59 \times 10^{10}$  vg/ml), AAV9 ABE8e - NT ( $8.93 \times 10^{10}$  vg/ml) and AAV9 ABE8e - CT ( $1.59 \times 10^{10}$  vg/ml). (Figure 1) All viral vectors were stored in deep freezer (-80°C).

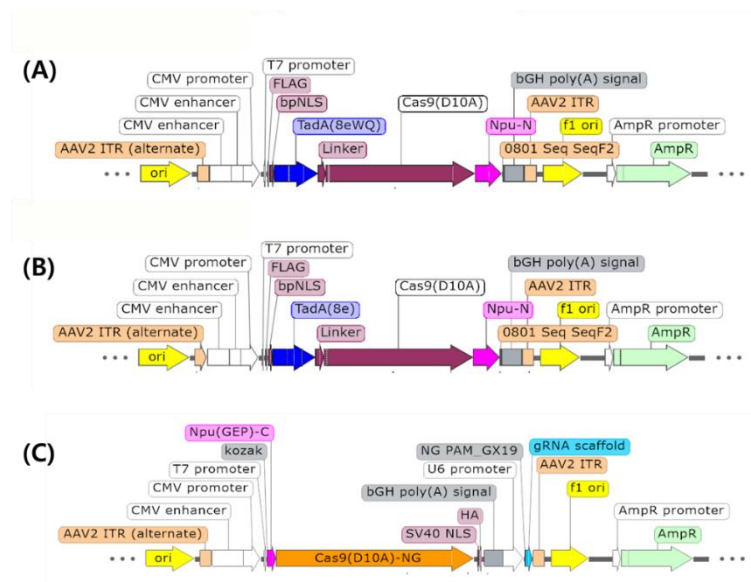


**Figure 1. Injection materials encoding adenine base editor (ABE).** The architecture of three types of adenine base editor used in this study. Split ABE8eWQ and ABE8e genes were with GX19 guide RNA. ABE8eWQ and ABE8e – NT, CT virus (VectorBuilder) was injected in both lateral ventricle sides of the pup’s brain. (A) ABE8eWQ-NT, (B) ABE8e-NT, (C) CT of both ABE8eWQ and ABE8e. ABE: adenine base editor, NT: N-terminal, CT: C-terminal.

## **2. Animals and animal welfare**

The mutant strain (B6.CE-Galc<sup>twi</sup>/J, JAX comprehensive protocol #000845) were supplied by Jackson Laboratory (USA) and maintained under specific pathogen-free conditions in this study. The Galc<sup>twi</sup> mutation involves G to A transition at codon 355 of GALC gene, creating a stop codon. They were kept on a 12 h/12 h inverted light cycle. For generating homozygous twitcher, we create mating cages using standard cages (27×22.5×14 cm<sup>3</sup>). All mice were genotyped before P21. The female to male ratio did not exceed 1:3. This study was approved by the Institutional Animal Care and Use Committee (IACUC) of Yonsei University Health System (permit number: 2020-0029, 2020-0047).

## **3. Neonatal stereotaxic surgery on postnatal day 1**

Stereotaxic viral delivery into brain was conducted on postnatal day 1. Newborn pups were cryoanesthetized during 1 min, and then injected with 1  $\mu$ l of viral preparation into both lateral ventricle (LV) (AAV9 ABE8eWQ and AAV9 ABE8e - NT, CT: 5  $\times$  10<sup>9</sup> vg, each) with a 32-G Hamilton syringe. We performed intracerebroventricular (ICV) injection to not only newborn Krabbe mouse but also wild-type mouse to evaluate the safety of injected materials. (Figure 2) After the treatments, the mice were returned to their home cage with their mother. All ICV injection followed stereotaxic coordinates: AP +1.5 mm from Lambda, ML +0.8/-0.8 mm from Lambda, and DV -1.5 mm from dura mater.

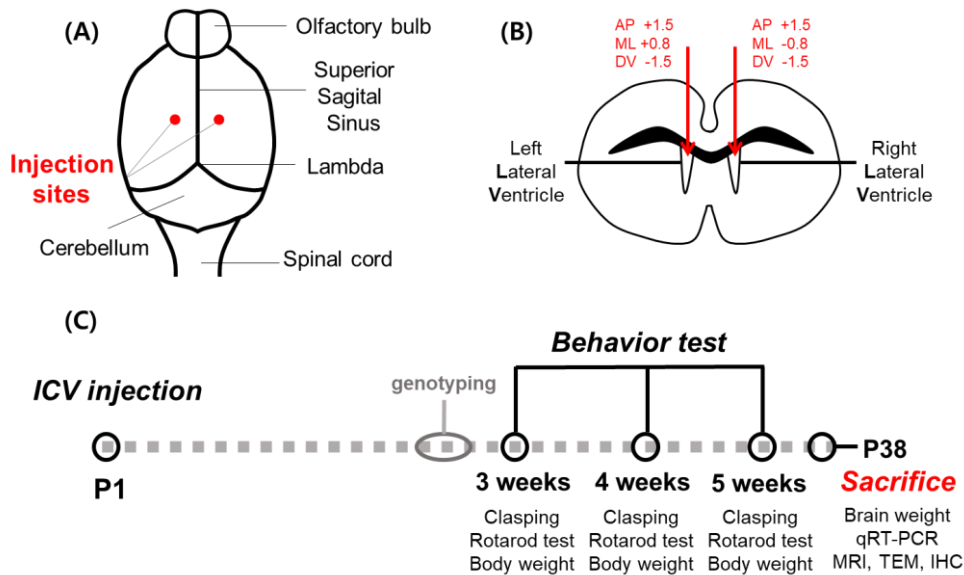


**Figure 2. The experimental scheme for animal model.** The intracerebroventricular injection of adenine base editor (ABE) were conducted on P1. Injection sites of the neonatal mouse were indicated. (A, B) The schedule for neonatal stereotaxic surgery and three times of behavioral assessment before mouse sacrifice on P38. To confirm the treatment effect of gene therapy using ABE, measurement of brain and body weight, rotarod test and clasping test were performed. (C) ABE, adenine base editor, P1: postnatal day 1, ICV: intracerebroventricular, qRT-PCR: quantitative reverse transcription polymerase chain reaction, MRI: magnetic resonance imaging, TEM: transmission electron microscope, IHC: immunohistochemistry.

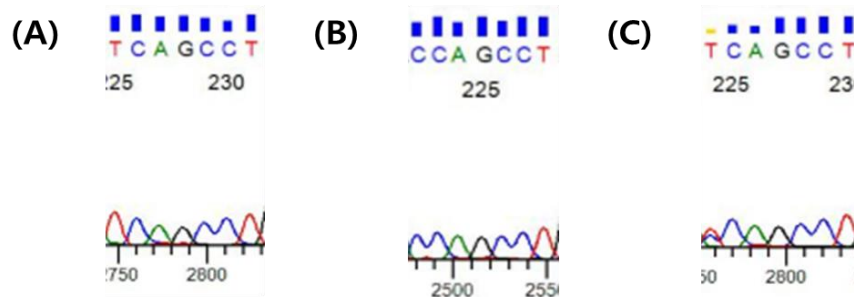


**Figure 3. Genotype for twitcher identification.** PCR-based genotyping of mouse. Genetic sequence of mouse with homozygous thymine; TCAGCCT (A), heterozygous thymine; TCAGCCT (B), homozygous cytosine; CCAGCCT. Mice which have homozygous thymine have disease phenotype, while mice which have heterozygous thymine or homozygous cytosine have normal phenotype.

#### 4. Behavioral assessments

After genotyping on P17-20, all behavioral test was conducted on P21, P28 and P35. (Figure 3, 4)

- 1) **Rotarod test:** Motor coordination and locomotor function were tested using rotarod test. Testing consists of three trials with intertrial intervals of 10 min. Mice were placed on the rolling rod (Ugo Basie, Gemonio (VA), Italy) and we measured the latency to fall of them as an indicator of this test before the maximum time was reached.
- 2) **Clasping test:** Functional impairments and locomotor asymmetry were tested using clasping test. Mice were suspended by their tail for 10 s to provoke a clasping phenotype which reflects hindlimb retraction. Results were scored based on the time taken to clasp: 0 = no clasping behavior, 1 = 1 to 5 seconds of clasping behavior, 2 = 5-10 seconds of clasping behavior, 3 = 10 seconds of clasping behavior. The score is an indicator of lesions in the motor pathway.

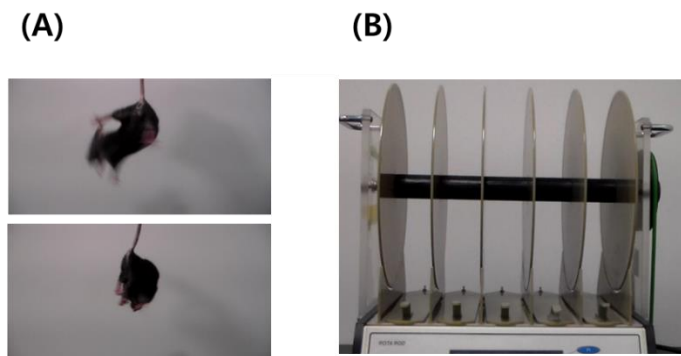


**Figure 4. Behavioral assessment.** Images of clasp test (A) and rotarod test (B).

### 5. Mouse sacrifice

Mice were anesthetized with 40~60  $\mu$ l katamine (0~50 mg/kg) and rompun mixed solution (10 ml: 0.67 ml = katamine: rompun) on the postnatal day 38. They were placed in dark and comfortable cage for more than 10 minutes to be sufficiently anesthetized. After cardiac perfusion with PBS, we harvested not only their brain but also the other abdominal organs: heart, liver, spinal cord and sciatic nerve. Organ samples for molecular study were stored in deep freezer (-80 °C) while those for histological study were stored in 30 % sucrose at 4 °C.

### 6. RNA isolation

RNA extraction was conducted using the TRIzol reagent (Invitrogen Life Technologies, Carlsbad, CA, U.S.A.) from in vivo samples. Isolated RNA samples were air dried in RT for 30 min to allow remaining washing solution to evaporate and resuspended in DEPC. Quantification of RNA was measured on Agilent 2100 Bioanalyzer (Agilent Technologies, Palo Alto, CA, U.S.A.) with the A260/A280 ratio which can be used to confirm the purity of RNA.

## 7. Quantitative real-time-polymerase chain reaction (qRT-PCR)

qRT-PCR was conducted in triplicate on StepOnePlus Real-Time PCR system (Applied Biosystems, Foster City, CA, U.S.A.) using 2xqPCRBIO SyGreen Mix (PB20.12-05, PCR Biosystems, London, UK), with thermocycler conditions as follows: amplifications start with a template preincubation step at 95 °C for 300 s, followed by 45 cycles at 95 °C for 10 s, 60 °C for 10 s, and 72 °C for 10 s. ABE8eWQ primers are as follows: NT, forward 5'-GGAATCCTGGCAGATGAATG-3' and reverse 5'-AAGAAGCTGTCGTCCACCTT-3'; CT, forward 5'-TGGGCAGCCAGATCCTGAA-3' and reverse 5'-CCGGATCAGCTTGTCATTCT-3'. ABE8e primers are as follows: NT, forward 5'-GGAATCCTGGCAGATGAATG-3' and reverse 5'-AAGAAGCTGTCGTCCACCTT-3'; CT, forward 5'-TGGGCAGCCAGATCCTGAA-3' and reverse 5'-CCGGATCAGCTTGTCATTCT-3'. Glyceraldehyde 3-phosphate dehydrogenase (GAPDH) primers are as follows: forward 5'-GTCGGTGTGAACGGATTTG-3' and reverse 5'-GAACATGTAGACCATGTAGTTG-3'.

## 8. High-throughput sequencing

This technology is used to determine the order of nucleotides in targeted regions of GALC gene. Genes were amplified from cDNA using SUN-PCR blend (Sun Genetics), purified using Expin PCR SV mini (GeneAll) and sequenced using a MiniSeq Sequencing System (Illumina). The results were finally analyzed by BE-Analyzer (<http://www.rgenome.net/be-analyzer/>) to confirm the base editing efficiency of each adenine base editor.

## 9. Immunofluorescence (IF)

The brain sample were frozen quickly in isopentane with dry ice, and sectioned into 16 µm thick using cryostat (Leica Microsystems, Austria). The coronal section of the

brain included corpus callosum area so that it can be immunohistochemically analyzed for myelin basic protein(MBP). We use anti-MBP (1:1000; Abcam) for primary antibody and Alexa Fluor® 594 goat anti-mouse (1:400; Invitrogen) for secondary antibody. Immunostained slides were covered with Vectashield® mounting medium with 4', 6-diamidino-2-phenylindole (DAPI; Vector, Burlingame, CA, U.S.A.) and analyzed using M2 microscopy (Zeiss, Gottingen, Germany).

#### **10. Hematoxylin and eosin staining**

Hematoxylin and eosin (H&E) staining is a well-established technique to examine pathological changes. We differentiated between the nuclear (purple) and cytoplasmic parts (pink) of in vivo tissue. The patterns of coloration showed the distribution of cells and provided a general overview of a histopathological structure. This experiment was conducted to determine whether there were any histological abnormalities like dysplasia.

#### **11. Luxol fast blue/ Periodic acid schiff staining**

LFB stains the myelin blue, and PAS stains demyelinated axons pink. Tissue samples including brain and spinal cord were fixed in 4 % paraformaldehyde at 4°C, embedded in paraffin wax. We used 4 µm paraffin-embedded coronal sections of corpus callosum region. Deparaffinized brain sections were incubated in Luxol Fast Blue Solution (0.1 %) at 70 °C for overnight. The sections were washed in tap water, and differentiated by dipping in 0.05 % Lithium Carbonate Solution and 70 % ethanol until the gray matter became transparent. After dehydration, all sections cleared by xylene mounted with mounting solution.

#### **12. Transmission electron microscopy (TEM)**

We reported on electron microscopy analysis of corpus callosum and sciatic nerve. Mouse brains were prepped at postnatal day 38 and immediately fixed in 0.1 M

phosphate buffer followed by 4% PFA containing 2% glutaraldehyde (MERCK, Darmstadt, Germany) for more than 12 hours. The samples were postfixed with 1% osmium tetroxide dissolved in 0.1 M phosphate buffer for 2 hours, dehydrated in ethanol and infiltrated with propylene oxide. Embedding solution was a Poly/Bed 812 kit (Polysciences, Warrington, PA, U.S.A). For counter staining, 70 nm thick ultra-thin slices were stained with 6 % uranyl acetate (EMS, 22,400 for 20 min) and lead citrate (Fisher, for 10 min). The brain samples are sectioned using a LEICA EM UC-7 (Leica Microsystems) and transferred onto copper and nickel grids. All sections were observed by a transmission electron microscope (JEM-1011, JEOL, Japan). The number of myelin turns and axons were measured after imaging.

### **13. DTI metric acquisition and comparison**

Mice were anesthetized with 1–2% isoflurane at postnatal day 38. The images were acquired using a 9.4 T Biospec scanner (Bruker, Ettlingen, Germany) running Paravision 5.1, using a 40 mm transceiver coil. Anatomical images were obtained according to the rapid acquisition with relaxation enhancement (RARE) protocol. Diffusion experiments were conducted using the diffusion tensor imaging (DTI) echo planar imaging (DTI-EPI) protocol and processed in DSI studio software (<http://dsi-studio.labsolver.org>). DTI data were analyzed in MATLAB (MathWorks, Natick, MA). Comparisons were then made between each group by four kinds of DTI parameters: FA, AD, RD and MD. The imaging parameters: slice thickness, 0.32 mm; number of slices, 20; matrix size, 128×128; matrix resolution, 0.156×0.156 mm; 4/10 ms; 30 directions with  $b = 670 \text{ s/mm}^2$ ; and TE/TR = 23.5/5000 ms.

### **14. Statistical analysis**

Data are shown as mean  $\pm$  standard error of the mean (SEM), and significant statistical differences were assessed using the one-way analysis of variance (ANOVA) followed by a post hoc Bonferroni and LSD comparison. Two-way repeated-measure

analysis of variance was also conducted to evaluate the interaction effect between time and group in rotarod test, and clasping test and measurement of mouse body weight. The statistical significant levels are given as follows:  $*p < 0.05$ ,  $**p < 0.01$ ,  $***p < 0.001$  in Bonferroni and  $^{\#}p < 0.05$ ,  $^{\#\#}p < 0.01$ ,  $^{\#\#\#}p < 0.001$  in LSD. We used Statistical Package for Social Sciences (SPSS) version 25.0 (IBM Corporation, Armonk, NY, USA) for statistical analysis. And all graphs were described in the Graph Pad Prism version 9.

### III. RESULTS

#### 1. mRNA expression of split ABEs was significantly higher in frontal cortex and corpus callosum

Genetic sequence of ABE8e and ABE8eWQ were divided and packaged in split AAV9 vectors and injected to twitcher on P1. ABE treated mice were sacrificed on P38 and mRNA was extracted from their brain and internal organs. We selected four specific brain regions for analysis, which were frontal cortex, corpus callosum, hippocampus and cerebellum. The mRNA of ABE –NT and CT was highly expressed around the viral injection sites and rarely expressed in the other brain regions. It seems AAV9 vectors reached frontal cortex and corpus callosum in relatively large numbers. (Figure 5) This means the mRNA expression levels represents distribution of AAV9 vectors *in vivo*.

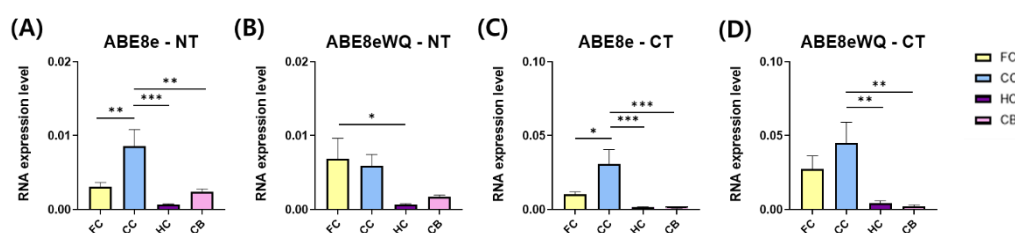


**Figure 5. RNA expression levels of viral vectors in four specific brain regions.** The mRNA expression levels show distribution of AAV9 viral vectors *in vivo*. N-terminal (A) and C-terminal (C) of ABE8e, and N-terminal (B) and C-terminal (D) of ABE8eWQ were shown. (Number of experimental samples from four mice; Untreated: n = 16, GFP: n = 16, ABE8e n = 16, ABE8eWQ: n = 16) The experimental samples were extracted from four specific brain regions: FC, CC, HC and CB. Data were analyzed using the one-way ANOVA and post-hoc comparisons (Bonferroni). The data are presented as mean  $\pm$  SEM. \* $p < 0.05$ , \*\* $p < 0.01$ , \*\*\* $p < 0.001$ . FC: frontal cortex, CC: corpus callosum, HC: hippocampus, CB: cerebellum.

**Table 1. Heterogeneity of variance information of mRNA expression in the four specific brain regions**

Region	ABE8e - NT	ABE8e - CT	ABE8eWQ - NT	ABE8eWQ - CT
FC	0.0031 ± 0.0006	0.0104 ± 0.0015	0.0098 ± 0.0040	0.0423 ± 0.0120
CC	0.0086 ± 0.0022	0.0308 ± 0.0098	0.0077 ± 0.0022	0.0641 ± 0.0188
HC	0.0007 ± 0.0001	0.0016 ± 0.0002	0.0008 ± 0.0001	0.0061 ± 0.0022
CB	0.0024 ± 0.0003	0.0008 ± 0.0001	0.0016 ± 0.0003	0.0031 ± 0.0013
<b>F-value</b>	8.817	7.931	3.785	7.139
<b>P-value</b>	< 0.001	< 0.001	0.017	0.001

Note : Data are presented as mean ± SEM. Statistical analysis were conducted using the one-way ANOVA and post-hoc comparisons (Bonferroni). ABE: adenine base editor, FC: frontal cortex, CC: corpus callosum, HC: hippocampus, CB: cerebellum.

**Table 2. Statistical information of mRNA expression in the four specific brain regions**

Split ABEs	Comparison regions			N	P-value	
ABE8e - NT	FC	vs.	CC	12 : 12	**	0.009
		vs.	HC	12 : 12	ns	0.872
		vs.	CB	12 : 12	ns	1.000
	CC	vs.	HC	12 : 12	***	< 0.001
		vs.	CB	12 : 12	**	0.003
		vs.	CB	12 : 12	ns	1.000
ABE8e -CT	FC	vs.	CC	12 : 12	*	0.035
		vs.	HC	12 : 12	ns	1.000

		vs.	CB	12 : 12	ns	1.000
	CC	vs.	HC	12 : 12	***	< 0.001
		vs.	CB	12 : 12	***	< 0.001
	HC	vs.	CB	12 : 12	ns	1.000
ABE8eWQ -NT	FC	vs.	CC	12 : 12	ns	1.000
		vs.	HC	12 : 12	*	0.048
		vs.	CB	12 : 12	ns	0.087
	CC	vs.	HC	12 : 12	ns	0.239
		vs.	CB	12 : 12	ns	0.398
	HC	vs.	CB	12 : 12	ns	1.000
ABE8eWQ -CT	FC	vs.	CC	10 : 12	ns	1.000
		vs.	HC	10 : 12	ns	0.188
		vs.	CB	10 : 12	ns	0.122
	CC	vs.	HC	12 : 12	**	0.003
		vs.	CB	12 : 12	**	0.002
	HC	vs.	CB	12 : 12	ns	1.000

Note : Data are presented as mean  $\pm$  SEM. Statistical analysis were conducted using the one-way ANOVA and post-hoc comparisons (Bonferroni). \* $p < 0.05$ , \*\* $p < 0.01$ , \*\*\* $p < 0.001$ , ns: non-significance. ABE: adenine base editor, FC: frontal cortex, CC: corpus callosum, HC: hippocampus, CB: cerebellum.

## 2. Adenine editing accuracy of ABE8eWQ was higher than that of ABE8e

When ABEs are injected to mouse brain, their gRNA guides the material into the editing window and attaches to the site so that the ABE can operate.<sup>13</sup> The editing window contains target adenine, but non-target adenines called bystanders are also distributed near it. (Figure 6) So, editing efficiency of target adenine and two bystanders is measured respectively. Through the high-throughput sequencing of cDNA, the conversion from the mutant adenine (A<sub>5</sub>) to the guanine was identified in both frontal cortex and corpus callosum in ABE treated groups compared to that in control groups. (Figure 7A) For editing efficiency of bystanders (A<sub>7</sub>, A<sub>10</sub>), however, we found statistically significant differences between ABE8e and ABE8eWQ. In conclusion, for base editing efficiency of targeted adenine (A<sub>5</sub>), ABE8e and ABE8eWQ showed a similar level of action, but for two bystander adenines (A<sub>7</sub>, A<sub>10</sub>), ABE8e showed significantly higher editing efficiency comparing to ABE8eWQ in frontal cortex and corpus callosum. It means that the base correction ability of ABE8eWQ is more sophisticated than that of ABE8e, suggesting that 8eWQ is more likely to be safer as an in vivo therapeutic than 8e. (Figure 7B, 7C)

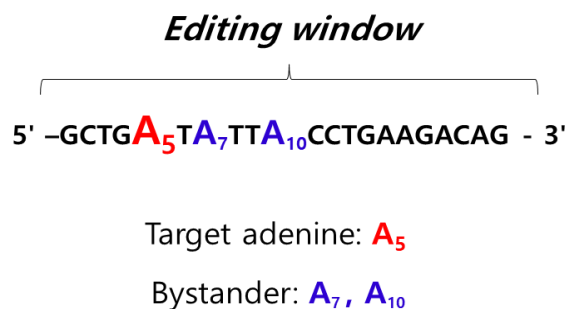


**Figure 6. Gene editing window of ABE8e and ABE8eWQ.** The sequence represents editing window of both ABE8e and ABE8eWQ. The target adenine we desire to edit using adenine base editors is A<sub>5</sub>. Two undesired editing spots in same editing window called bystander are A<sub>7</sub> and A<sub>10</sub>. ABE: adenine base editor.

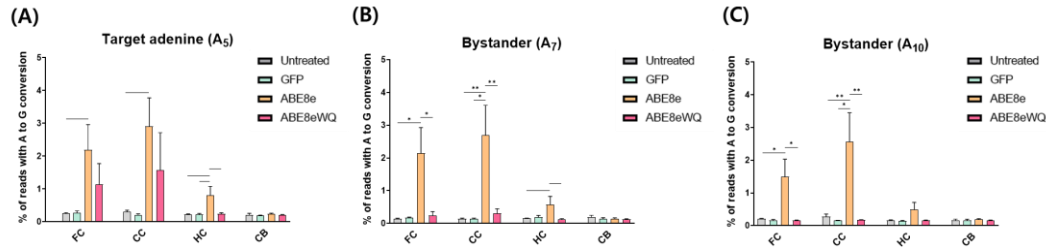


**Figure 7. Gene editing efficiency of ABE8e and ABE8eWQ in four brain regions.** Percentage of adenine conversion for evaluating the efficiencies and outcomes of base editing. Graphs show the base substitution activity of each ABE on A<sub>5</sub> (A) which is a target adenine, A<sub>7</sub> (B) and A<sub>10</sub> (C) which are bystanders. (Untreated: n = 6, GFP: n = 3, ABE8e n = 6, ABE8eWQ: n = 6) The experimental samples were extracted from four specific brain regions: FC, CC, HC and CB. Data were analyzed using the one-way ANOVA and post-hoc comparisons (Bonferroni and LSD). The data are presented as mean ± SEM. \**p* < 0.05, \*\**p* < 0.01, \*\*\**p* < 0.001 in Bonferroni and #*p* < 0.05, ##*p* < 0.01, ###*p* < 0.001 in LSD. ABE: adenine base editor, GFP: green fluorescent protein, FC: frontal cortex, CC: corpus callosum, HC: hippocampus, CB: cerebellum

**Table 3. Heterogeneity of variance information of gene editing efficiency of target adenine (A<sub>5</sub>)**

Region	Frontal cortex	Corpus callosum	Hippocampus	Cerebellum
Untreated	0.2617 ± 0.0194	0.3033 ± 0.0490	0.2267 ± 0.0117	0.2117 ± 0.439
GFP	0.2767 ± 0.0555	0.2133 ± 0.0318	0.2267 ± 0.0260	0.1967 ± 0.0033
ABE8e	2.1917 ± 0.7702	2.9080 ± 0.8662	0.8150 ± 0.2662	0.2360 ± 0.0223
ABE8eWQ	1.1483 ± 0.6231	1.5800 ± 1.1347	0.2400 ± 0.0318	0.1983 ± 0.0170
<b>F-value</b>	2.575	2.273	3.815	0.328
<b>P-value</b>	0.088	0.119	0.029	0.805

Note : Data are presented as mean  $\pm$  SEM. Statistical analysis were conducted using the one-way ANOVA and post-hoc comparisons (Bonferroni). ABE: adenine base editor, GFP: green fluorescent protein.

**Table 4. Heterogeneity of variance information of gene editing efficiency of bystander adenine (A<sub>7</sub>)**

<b>Region</b>	<b>Frontal cortex</b>	<b>Corpus callosum</b>	<b>Hippocampus</b>	<b>Cerebellum</b>
Untreated	0.1450 $\pm$ 0.0134	0.1400 $\pm$ 0.0205	0.1550 $\pm$ 0.0099	0.1900 $\pm$ 0.0597
GFP	0.1700 $\pm$ 0.0208	0.1433 $\pm$ 0.0186	0.1833 $\pm$ 0.0601	0.1467 $\pm$ 0.0296
ABE8e	2.1417 $\pm$ 0.7838	2.6940 $\pm$ 0.9138	0.5733 $\pm$ 0.2523	0.1440 $\pm$ 0.0256
ABE8eWQ	0.2400 $\pm$ 0.1206	0.3083 $\pm$ 0.1379	0.1317 $\pm$ 0.0151	0.1267 $\pm$ 0.0131
<b><i>F</i>-value</b>	4.920	7.182	2.244	0.527
<b><i>P</i>-value</b>	0.012	0.003	0.120	0.670

Note : Data are presented as mean  $\pm$  SEM. Statistical analysis were conducted using the one-way ANOVA and post-hoc comparisons (Bonferroni). ABE: adenine base editor, GFP: green fluorescent protein.

**Table 5. Heterogeneity of variance information of gene editing efficiency of bystander adenine (A<sub>10</sub>)**

<b>Region</b>	<b>Frontal cortex</b>	<b>Corpus callosum</b>	<b>Hippocampus</b>	<b>Cerebellum</b>
Untreated	0.2050 $\pm$ 0.0138	0.2750 $\pm$ 0.0802	0.1633 $\pm$ 0.0131	0.1633 $\pm$ 0.0364
GFP	0.1533 $\pm$ 0.0348	0.1567 $\pm$ 0.0088	0.1467 $\pm$ 0.0120	0.1567 $\pm$ 0.0393
ABE8e	1.4950 $\pm$ 0.5384	2.5620 $\pm$ 0.8885	0.4967 $\pm$ 0.2118	0.1980 $\pm$ 0.0128

ABE8eWQ	0.1550 ± 0.0177	0.1683 ± 0.0135	0.1617 ± 0.0091	0.1617 ± 0.0111
<b>F-value</b>	4.863	6.943	2.044	0.489
<b>P-value</b>	0.013	0.003	0.146	0.695

Note : Data are presented as mean ± SEM. Statistical analysis were conducted using the one-way ANOVA and post-hoc comparisons (Bonferroni). ABE: adenine base editor, GFP: green fluorescent protein.

**Table 6. Statistical information of gene editing efficiency of target adenine (A<sub>5</sub>)**

Region	Comparison regions		N		P-value
Frontal cortex	Untreated	vs. GFP	6 : 3	ns	1.000
		vs. ABE8e	6 : 6	ns	0.127
		vs. ABE8eWQ	6 : 6	ns	1.000
	GFP	vs. ABE8e	3 : 6	ns	0.332
		vs. ABE8eWQ	3 : 6	ns	1.000
		ABE8e vs. ABE8eWQ	6 : 6	ns	1.000
Corpus callosum	Untreated	vs. GFP	6 : 3	ns	1.000
		vs. ABE8e	6 : 5	ns	0.192
		vs. ABE8eWQ	6 : 6	ns	1.000
	GFP	vs. ABE8e	3 : 5	ns	0.367
		vs. ABE8eWQ	3 : 6	ns	1.000
		ABE8e vs. ABE8eWQ	5 : 6	ns	1.000
Hippocampus	Untreated	vs. GFP	6 : 3	ns	1.000
		vs. ABE8e	6 : 6	ns	0.066
		vs. ABE8eWQ	6 : 6	ns	1.000
	GFP	vs. ABE8e	3 : 6	ns	0.194

		vs. ABE8eWQ	3 : 6	ns	1.000
	ABE8e	vs. ABE8eWQ	6 : 6	ns	0.075
Cerebellum	Untreated	vs. GFP	6 : 3	ns	1.000
		vs. ABE8e	6 : 5	ns	1.000
		vs. ABE8eWQ	6 : 6	ns	1.000
	GFP	vs. ABE8e	3 : 5	ns	1.000
		vs. ABE8eWQ	3 : 6	ns	1.000
		ABE8e vs. ABE8eWQ	5 : 6	ns	1.000

Note : Data are presented as mean  $\pm$  SEM. Statistical analysis were conducted using the one-way ANOVA and post-hoc comparisons (Bonferroni). \* $p < 0.05$ , \*\* $p < 0.01$ , \*\*\* $p < 0.001$ , ns: non-significance. ABE: adenine base editor, GFP: green fluorescent protein.

**Table 7. Statistical information of gene editing efficiency of bystander adenine (A<sub>7</sub>)**

Region	Comparison regions		N		P-value
Frontal cortex	Untreated	vs. GFP	6 : 3	ns	1.000
		vs. ABE8e	6 : 6	*	0.026
		vs. ABE8eWQ	6 : 6	ns	1.000
	GFP	vs. ABE8e	3 : 6	ns	0.102
		vs. ABE8eWQ	3 : 6	ns	1.000
		ABE8e vs. ABE8eWQ	6 : 6	*	0.037
Corpus callosum	Untreated	vs. GFP	6 : 3	ns	1.000
		vs. ABE8e	6 : 5	**	0.005
		vs. ABE8eWQ	6 : 6	ns	1.000
	GFP	vs. ABE8e	3 : 5	*	0.024
		vs. ABE8eWQ	3 : 6	ns	1.000

	ABE8e	vs.	ABE8eWQ	5 : 6	**	0.010		
Hippocampus	Untreated	vs.	GFP	6 : 3	ns	1.000		
			ABE8e	6 : 6	ns	0.281		
			ABE8eWQ	6 : 6	ns	1.000		
	GFP	vs.	ABE8e	3 : 6	ns	0.726		
			ABE8eWQ	3 : 6	ns	1.000		
	Cerebellum	Untreated	vs.	ABE8e	6 : 6	ns	0.222	
GFP				vs.	GFP	6 : 3	ns	1.000
					ABE8e	6 : 5	ns	1.000
GFP		vs.	ABE8eWQ	6 : 6	ns	1.000		
			ABE8e	vs.	ABE8e	3 : 5	ns	1.000
ABE8e		vs.			ABE8eWQ	3 : 6	ns	1.000
	ABE8e		vs.	ABE8eWQ	5 : 6	ns	1.000	

Note : Data are presented as mean  $\pm$  SEM. Statistical analysis were conducted using the one-way ANOVA and post-hoc comparisons (Bonferroni). \* $p < 0.05$ , \*\* $p < 0.01$ , \*\*\* $p < 0.001$ , ns: non-significance. ABE: adenine base editor, GFP: green fluorescent protein.

**Table 8. Statistical information of gene editing efficiency of bystander adenine (A<sub>10</sub>)**

Region	Comparison regions		N		P-value	
Frontal cortex	Untreated	vs.	GFP	6 : 3	ns	1.000
			ABE8e	6 : 6	*	0.037
			ABE8eWQ	6 : 6	ns	1.000
	GFP	vs.	ABE8e	3 : 6	ns	0.101
			ABE8eWQ	3 : 6	ns	1.000
	ABE8e	vs.	ABE8eWQ	6 : 6	*	0.029

Corpus callosum	Untreated	vs. GFP	6 : 3	ns	1.000
		vs. ABE8e	6 : 5	**	0.010
		vs. ABE8eWQ	6 : 6	ns	1.000
	GFP	vs. ABE8e	3 : 5	*	0.027
		vs. ABE8eWQ	3 : 6	ns	1.000
		ABE8e vs. ABE8eWQ	5 : 6	**	0.007
Hippocampus	Untreated	vs. GFP	6 : 3	ns	1.000
		vs. ABE8e	6 : 6	ns	0.339
		vs. ABE8eWQ	6 : 6	ns	1.000
	GFP	vs. ABE8e	3 : 6	ns	0.585
		vs. ABE8eWQ	3 : 6	ns	1.000
		ABE8e vs. ABE8eWQ	6 : 6	ns	0.333
Cerebellum	Untreated	vs. GFP	6 : 3	ns	1.000
		vs. ABE8e	6 : 5	ns	1.000
		vs. ABE8eWQ	6 : 6	ns	1.000
	GFP	vs. ABE8e	3 : 5	ns	1.000
		vs. ABE8eWQ	3 : 6	ns	1.000
		ABE8e vs. ABE8eWQ	5 : 6	ns	1.000

Note : Data are presented as mean  $\pm$  SEM. Statistical analysis were conducted using the one-way ANOVA and post-hoc comparisons (Bonferroni). \* $p < 0.05$ , \*\* $p < 0.01$ , \*\*\* $p < 0.001$ , ns: non-significance. ABE: adenine base editor, GFP: green fluorescent protein.

### 3. Both ABE8e and ABE8eWQ preserved weight loss of twitcher mice

The signs of Krabbe disease include severe seizures, tremors, weight loss, muscle stiffness and pelvic limb paralysis.<sup>14,15</sup> But affected mouse shows no neurological deficits until postnatal day 20. Thus we decided to conduct behavioral test on P21, P28 and P35 and compare the scores of each group.

To evaluate the clinical effect of the base editing, the body weight of all mice was measured three times on P21, P28 and P35, and the brain weight was measured right after the mouse was sacrificed on P38. The body weight of ABE8e and ABE8eWQ groups was significantly higher than that of control groups and there was also a significant interaction between time and group ( $p < 0.001$ ). (Figure 8A, 8B) ABE8e and ABE8eWQ groups showed significantly increased brain weight compared to that in control groups. (Figure 8C)

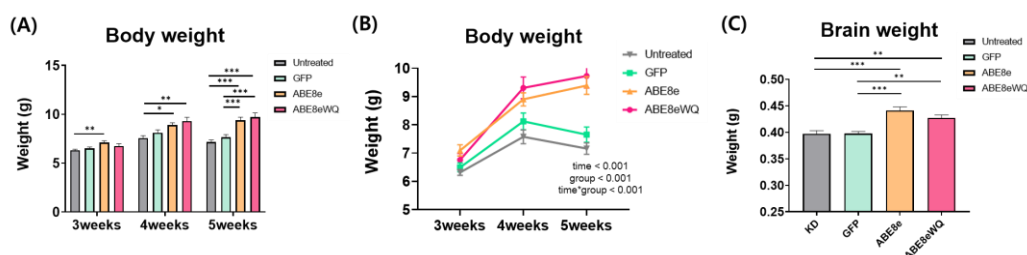


**Figure 8. Body weights and brain weights in twitcher groups.** (A, B) The measurement of body weight (Untreated:  $n = 44$ , GFP:  $n = 41$ , ABE8e  $n = 20$ , ABE8eWQ:  $n = 20$ ) (C) The measurement of whole brain weight of mouse on postnatal day 38 (Untreated:  $n = 22$ , GFP:  $n = 25$ , ABE8e  $n = 23$ , ABE8eWQ:  $n = 17$ ) The data are presented as mean  $\pm$  SEM. The statistics used for the bar graph were the one-way ANOVA (Bonferroni), whereas the statistics used for the line graph were two-way ANOVA which is used to estimate how the mean of a quantitative variable changes according to the levels of two categorical variables, the time and disease conditions.  $*p < 0.05$ ,  $**p < 0.01$ ,  $***p < 0.001$ . ABE: adenine base editor, GFP: green fluorescent protein.

**Table 9. Heterogeneity of variance information of body weight and brain weight**

Test	Week	Untreated	GFP	ABE8e	ABE8eWQ	F-value	P-value
Body weight	3	6.3 ± 0.1	6.5 ± 0.2	7.1 ± 0.2	6.8 ± 0.2	4.024	0.009
	4	7.6 ± 0.2	8.1 ± 0.3	8.9 ± 0.2	9.3 ± 0.4	6.254	< 0.001
	5	7.2 ± 0.2	7.7 ± 0.3	9.4 ± 0.3	9.7 ± 0.4	17.804	< 0.001
Brain weight		0.40 ± 0.006	0.40 ± 0.004	0.43 ± 0.005	0.44 ± 0.007	16.119	< 0.001

Note : Data are presented as mean ± SEM. Statistical analysis were conducted using the one-way ANOVA and post-hoc comparisons (Bonferroni). ABE: adenine base editor, GFP: green fluorescent protein.

**Table 10. Statistical information of body weight and brain weight**

		Comparison regions		N	P-value	
Body weight	Untreated	vs.	GFP	44 : 41	ns	0.922
		vs.	ABE8e	44 : 20	***	< 0.001
		vs.	ABE8eWQ	44 : 20	***	< 0.001
	GFP	vs.	ABE8e	41 : 20	***	< 0.001
		vs.	ABE8eWQ	41 : 20	***	< 0.001
		vs.	ABE8e	20 : 20	ns	1.000
Brain weight	Untreated	vs.	GFP	22 : 25	ns	1.000
		vs.	ABE8e	22 : 23	**	0.004
		vs.	ABE8eWQ	22 : 17	***	< 0.001
	GFP	vs.	ABE8e	25 : 23	**	0.003
		vs.	ABE8eWQ	25 : 17	***	< 0.001
		vs.	ABE8e	23 : 17	ns	0.599

Note : Data are presented as mean  $\pm$  SEM. Statistical analysis were conducted using the one-way ANOVA and post-hoc comparisons (Bonferroni). \* $p < 0.05$ , \*\* $p < 0.01$ , \*\*\* $p < 0.001$ , ns: non-significance. ABE: adenine base editor, GFP: green fluorescent protein.

#### **4. Both ABE8e and ABE8eWQ ameliorated neurobehavioral impairments of twitcher mice**

All mice were subjected to two behavioral tests during 3–5 weeks. The locomotor function and neuromuscular function of twitcher were evaluated using rotarod test and clasping test. In both behavior test, not only the one-way ANOVA but also the two-way ANOVA were used to prove clinical improvement effect of ABE8e and ABE8eWQ. In the clasping test, the symptoms of twitchers were alleviated in ABE8e and ABE8eWQ group compared to those of control groups, and there was a significant interaction effect between time and group ( $p < 0.001$ ). (Figure 9)

Rotarod test was performed under three speed conditions. First, mice were tested at constant speed of 4 rpm in a rotarod apparatus and the latency to fall within 5 min was recorded. Both ABE8e and ABE8eWQ group showed significant improvements compared to control groups and significant interactions effect occurs between time and group ( $p = 0.004$ ). (Figure 10) Second, mice were tested at constant speed of 12 rpm in a rotarod apparatus and the latency to fall within 30 sec was recorded. The same statistical results were shown under this condition. Both ABE8e and ABE8eWQ group showed significant improvements compared to control groups and significant interactions effect occurs between time and group ( $p = 0.039$ ). (Figure 11) Lastly, mice were tested at accelerating speeds of 4 rpm to 12 rpm and the latency to fall within 1 min was recorded. Significant differences were also observed between ABE treated groups and control groups. Interaction effect also occurs between time and group ( $p = 0.002$ ) (Figure 12)

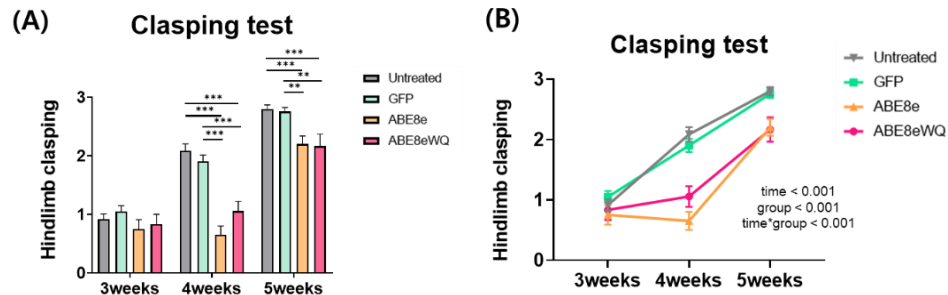


**Figure 9. Clasp test in twitcher groups.** Duration time of limb clasping under 10 seconds of tail-suspension was monitored. (Untreated: n = 35, GFP: n = 41, ABE8e n = 20, ABE8eWQ: n = 18) The data are presented as mean  $\pm$  SEM. The statistics used for the bar graph (A) were the one-way ANOVA (Bonferroni), whereas the statistics used for the line graph (B) were two-way ANOVA which is used to estimate how the mean of a quantitative variable changes according to the levels of two categorical variables, the time and disease conditions. \* $p < 0.05$ , \*\* $p < 0.01$ , \*\*\* $p < 0.001$ . ABE: adenine base editor, GFP: green fluorescent protein.

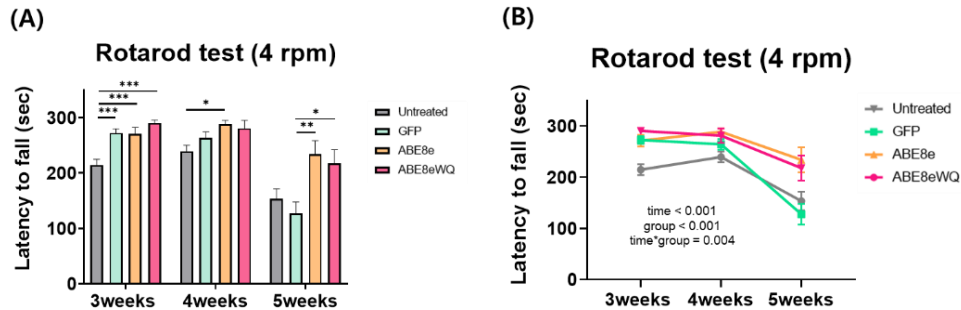


**Figure 10. Rotarod scores in twitcher groups (4 rpm).** Mice were tested at constant speed (4 rpm) in a rotarod apparatus. The latency time to fall from the rolling rod within 5 min was recorded. (Untreated: n = 40, GFP: n = 40, ABE8e n = 20, ABE8eWQ: n = 21) The data are presented as mean  $\pm$  SEM. The statistics used for the bar graph (A) were the one-way ANOVA (Bonferroni), whereas the statistics used for the line graph (B) were two-way ANOVA which is used to estimate how the mean of a quantitative variable changes according to the levels of two categorical variables, the time and disease conditions. \* $p < 0.05$ , \*\* $p < 0.01$ , \*\*\* $p < 0.001$ . ABE: adenine base editor, GFP: green fluorescent protein.

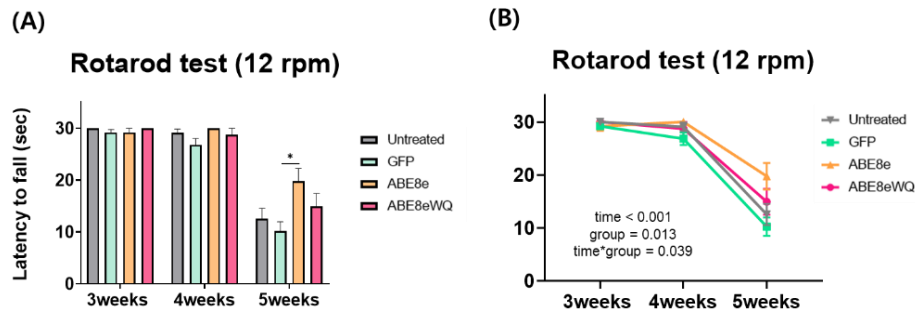


**Figure 11. Rotarod scores in twitcher groups (12 rpm).** Mice were tested at constant speed (12 rpm) in a rotarod apparatus. The latency time to fall from the rolling rod within 30 sec was recorded. (Untreated: n = 40, GFP: n = 40, ABE8e n = 20, ABE8eWQ: n = 21) The data are presented as mean  $\pm$  SEM. The statistics used for the bar graph (A) were the one-way ANOVA (Bonferroni), whereas the statistics used for the line graph (B) were two-way ANOVA which is used to estimate how the mean of a quantitative variable changes according to the levels of two categorical variables, the time and disease conditions. \* $p < 0.05$ , \*\* $p < 0.01$ , \*\*\* $p < 0.001$ . ABE: adenine base editor, GFP: green fluorescent protein.

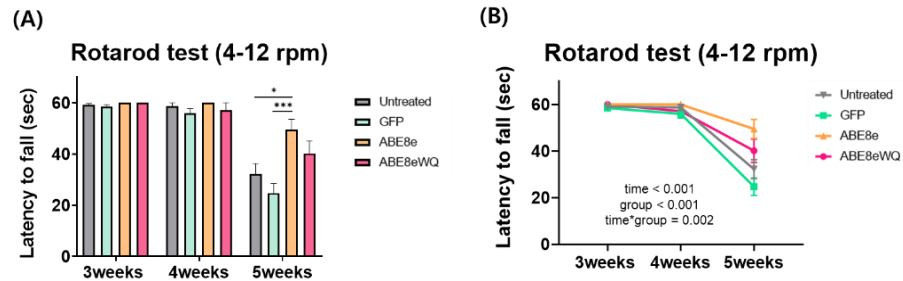


**Figure 12. Rotarod scores in twitcher groups (4-12 rpm).** Mice were tested at accelerating speed (from 4 to 12 rpm) in a rotarod apparatus. The latency time to fall from the rolling rod within 60 sec was recorded. (Untreated: n = 40, GFP: n = 40, ABE8e n = 20, ABE8eWQ: n = 21) The data are presented as mean  $\pm$  SEM. The statistics used for the bar graph (A) were the one-way ANOVA (Bonferroni), whereas the statistics used for the line graph (B) were two-way ANOVA which is used to estimate how the mean of a quantitative variable changes according to the levels of two categorical variables, the time and disease conditions. \* $p < 0.05$ , \*\* $p < 0.01$ , \*\*\* $p < 0.001$ . ABE: adenine base editor, GFP: green fluorescent protein.

**Table 11. Heterogeneity of variance information of the behavioral assessment in twitcher mice**

Test	Week	Untreated	GFP	ABE8e	ABE8eWQ	<i>F</i> -value	<i>P</i> -value
Clasping	3	0.9 ± 0.1	1.0 ± 0.1	0.8 ± 0.2	0.8 ± 0.2	1.139	0.337
	4	2.1 ± 0.1	1.9 ± 0.1	1.1 ± 0.2	0.7 ± 0.2	24.098	< 0.001
	5	2.8 ± 0.1	2.8 ± 0.1	2.2 ± 0.2	2.2 ± 0.1	9.963	< 0.001
Rotarod constant (4 rpm)	3	214.6 ± 10.5	272.6 ± 7.6	271.2 ± 11.3	290.3 ± 5.5	13.117	< 0.001
	4	239.4 ± 10.7	264.0 ± 10.3	288.6 ± 6.6	281.0 ± 14.0	3.726	0.013
	5	153.4 ± 18.2	127.5 ± 20.4	233.9 ± 24.4	217.7 ± 24.3	5.055	0.003
Rotarod constant (12 rpm)	3	30.0 ± 0.0	29.2 ± 0.6	29.2 ± 0.9	30.0 ± 0.0	0.821	0.485
	4	29.1 ± 0.8	26.8 ± 1.2	30.0 ± 0.0	28.7 ± 1.3	1.721	0.167
	5	12.6 ± 2.0	10.2 ± 1.7	19.8 ± 2.5	15.0 ± 2.5	3.531	0.017
Rotarod accelerated (4-12 rpm)	3	59.1 ± 0.6	58.5 ± 0.7	60.0 ± 0.0	60.0 ± 0.0	1.325	0.270
	4	58.7 ± 1.3	56.0 ± 1.8	60.0 ± 0.0	57.2 ± 2.9	1.016	0.388
	5	32.3 ± 4.0	24.7 ± 3.7	49.5 ± 4.1	40.2 ± 4.9	5.840	< 0.001

Note : Data are presented as mean ± SEM. Statistical analysis were conducted using the one-way ANOVA and post-hoc comparisons (Bonferroni). ABE: adenine base editor, GFP: green fluorescent protein.

**Table 12. Statistical information of the behavioral assessment in twitcher mice**

		Comparison regions		N	<i>P</i> -value	
Clasping	Untreated	vs.	GFP	35 : 41	ns	1.000
		vs.	ABE8e	35 : 20	***	< 0.001
		vs.	ABE8eWQ	35 : 18	***	< 0.001
	GFP	vs.	ABE8e	41 : 20	**	0.002
		vs.	ABE8eWQ	41 : 18	**	0.001
	ABE8e	vs.	ABE8eWQ	20 : 18	ns	1.000
Rotarod constant (4 rpm)	Untreated	vs.	GFP	40 : 40	ns	1.000
		vs.	ABE8e	40 : 20	ns	0.087
		vs.	ABE8eWQ	40 : 21	ns	0.277
	GFP	vs.	ABE8e	40 : 20	**	0.008
		vs.	ABE8eWQ	40 : 21	*	0.033
	ABE8e	vs.	ABE8eWQ	20 : 21	ns	1.000
Rotarod constant (12 rpm)	Untreated	vs.	GFP	29 : 41	ns	1.000
		vs.	ABE8e	29 : 20	ns	0.160
		vs.	ABE8eWQ	29 : 21	ns	1.000
	GFP	vs.	ABE8e	41 : 20	*	0.012
		vs.	ABE8eWQ	41 : 21	ns	0.685
	ABE8e	vs.	ABE8eWQ	20 : 21	ns	0.998
Rotarod accelerated (4-12 rpm)	Untreated	vs.	GFP	37 : 41	ns	0.896
		vs.	ABE8e	37 : 20	*	0.047
		vs.	ABE8eWQ	37 : 20	ns	1.000
	GFP	vs.	ABE8e	41 : 20	***	< 0.001
		vs.	ABE8eWQ	41 : 20	ns	0.090

---

ABE8e	vs.	ABE8eWQ	20 : 20	ns	1.000
-------	-----	---------	---------	----	-------

---

Note : Data are presented as mean  $\pm$  SEM. Statistical analysis were conducted using the one-way ANOVA and post-hoc comparisons (Bonferroni). \* $p < 0.05$ , \*\* $p < 0.01$ , \*\*\* $p < 0.001$  or ns: non-significance. ABE: adenine base editor, GFP: green fluorescent protein.

### **5. Both ABE8e and ABE8eWQ increased the lifespan of twitcher mice**

Twitcher have an obviously shortened lifespan compared to wild-type mice. To determine the effect of ABE treatment on lifespan extension, the median lifespan of all groups were measured. Treatment of ABE8e and ABE8eWQ significantly increased the median lifespan approximately 20 % compared to that in control groups. (Figure 13A) Kaplan–Meier curves showed the survival of various treatment groups. The median lifespan of ABE8e (44 d; range, 39-47 d) and ABE8eWQ (43 d; range, 42-43 d) group were significantly greater than that of the untreated (36 d; range, 34-44 d) group or GFP (36 d; range, 34-37 d) group. (Figure 13B) The interval survival rate of the Kaplan–Meier curve also showed the significant difference on P35 to P47, continuously. (Figure 13C).

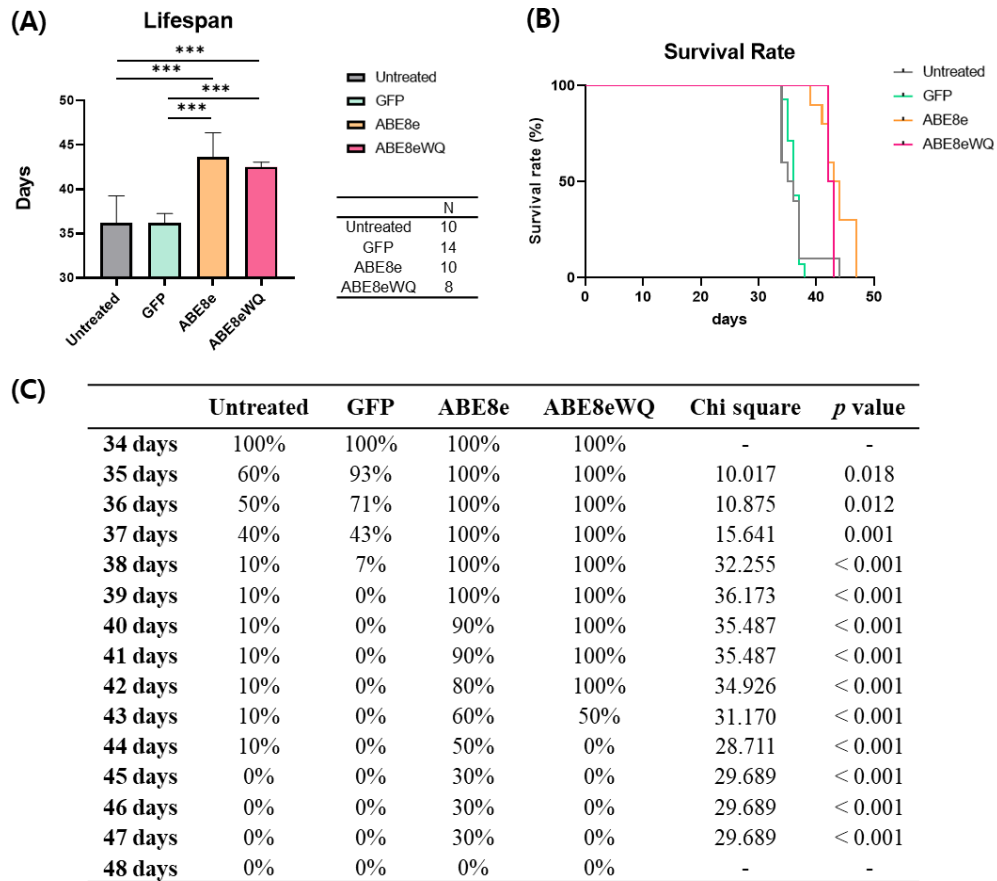


**Figure 13. Lifespan and survival rate.** Lifespan increasement (A) and survival rate of Kaplan-Meier curve (B) were shown. The interval survival rate of Kaplan-Meier curve was analyzed from P34 to P48. (C) (Untreated:  $n = 10$ , GFP:  $n = 14$ , ABE8e  $n = 10$ , ABE8eWQ:  $n = 8$ ) Data were analyzed using the one-way ANOVA and post-hoc comparisons (Bonferroni). The data are presented as mean  $\pm$  SEM. \* $p < 0.05$ , \*\* $p < 0.01$ , \*\*\* $p < 0.001$ . ABE: adenine base editor, GFP: green fluorescent protein.

#### **6. Both ABE8e and ABE8eWQ increased the expression of myelin basic protein in corpus callosum of twitcher mice**

Myelin basic protein (MBP) is an important protein especially in the process of myelination of nerves in the nervous system. This protein maintains the intact structure of myelin, interacting with the lipids in the myelin membrane.<sup>16</sup> Previous studies have been reported that demyelination in the central nervous system (CNS) were induced by reduction of MBP expression and resulted in tremors, seizures, and early death.<sup>17</sup>

To confirm the recovery of myelin sheath caused by ABE8e and ABE8eWQ, immunostaining of MBP was performed. MBP-positive cells were located along the corpus callosum under fluorescent microscopy in paraffin sections of the brains 38 days after injection. (Figure 14A, 14B) In the corpus callosum, MBP stain ratio in the ABE treated groups was higher than that in control groups. This means the myelin density and thickness of corpus callosum of the ABE treated groups were higher and thicker than those in control groups. (Figure 14C, 14D)

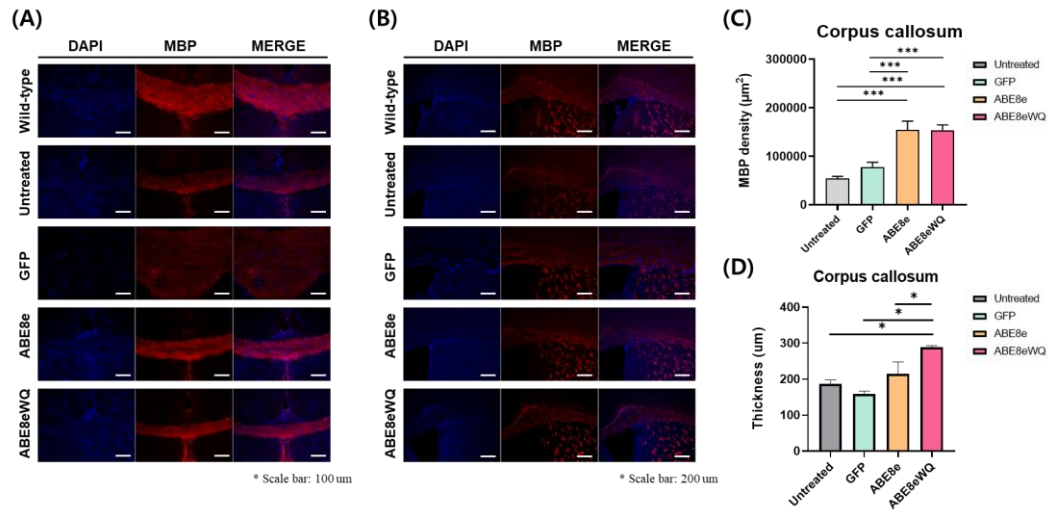


**Figure 14. Immunohistochemical expression of myelin basic protein (MBP).** MBP (red) and DAPI (blue) staining in center part (A) and lateral part (B) of the corpus callosum. MBP expression level represents myelin integrity. Each graph shows MBP density (C) and thickness of corpus callosum (D). (Number of experimental samples in MBP density from four mice; Untreated: n = 15, GFP: n = 15, ABE8e n = 16, ABE8eWQ: n = 15) (Number of experimental samples in thickness of corpus callosum; Untreated: n = 16 from four mice, GFP: n = 11 from three mice, ABE8e n = 14 from four mice, ABE8eWQ: n = 4 from one mouse) Data were analyzed using the one-way ANOVA and post-hoc comparisons (Bonferroni). The data are presented as mean ± SEM. \* $p < 0.05$ , \*\* $p < 0.01$ , \*\*\* $p < 0.001$ . ABE: adenine base editor, GFP: green fluorescent protein. (A) Scale bar: 100 µm, (B) Scale bar: 200 µm.

**Table 13. Heterogeneity of variance information of myelin basic protein expression**

Test		Untreated	GFP	ABE8e	ABE8eWQ	F-value	P-value
IHC	Density	54316 ± 4468	54316 ± 9760	54316 ± 17723	54316 ± 10987	19.537	< 0.001
	Thickness	178 ± 9.65	173 ± 7.49	182 ± 25.99	285 ± 2.38	3.840	0.016

Note : Data are presented as mean ± SEM. Statistical analysis were conducted using the one-way ANOVA and post-hoc comparisons (Bonferroni). IHC: immunohistochemistry ABE: adenine base editor, GFP: green fluorescent protein.

**Table 14. Statistical information of myelin basic protein expression**

		Comparison regions		N	P-value	
Density	Untreated	vs.	GFP	15 : 15	ns	0.952
		vs.	ABE8e	15 : 15	***	< 0.001
		vs.	ABE8eWQ	15 : 15	***	< 0.001
	GFP	vs.	ABE8e	15 : 15	***	< 0.001
		vs.	ABE8eWQ	15 : 15	***	< 0.001
	ABE8e	vs.	ABE8eWQ	15 : 15	ns	1.000
Thickness	Untreated	vs.	GFP	16 : 11	ns	1.000
		vs.	ABE8e	16 : 14	ns	1.000
		vs.	ABE8eWQ	16 : 4	*	0.017
	GFP	vs.	ABE8e	11 : 14	ns	1.000
		vs.	ABE8eWQ	11 : 4	*	0.018
	ABE8e	vs.	ABE8eWQ	14 : 4	*	0.028

Note : Data are presented as mean  $\pm$  SEM. Statistical analysis were conducted using the one-way ANOVA and post-hoc comparisons (Bonferroni). \* $p < 0.05$ , \*\* $p < 0.01$ , \*\*\* $p < 0.001$ , ns: non-significance. ABE: adenine base editor, GFP: green fluorescent protein.

**7. Both ABE8e and ABE8eWQ restored myelination in the corpus callosum, but not myelination in the sciatic nerve.**

Transmission Electron Microscopy (TEM) have been used to visualize myelinated fibers in the corpus callosum and sciatic nerve. As a result of observing the structure of myelin in corpus callosum using TEM, it was confirmed that there was a difference in the number of turns of myelin sheaths. Since the myelin sheath is a multi-layered membrane, which functions as an insulator to increase the velocity of axonal impulse conduction, the number of turns of myelin sheaths is a good indicator to evaluate the function of myelin.<sup>18</sup> ABE treated groups have approximately 2.5 additional turns of myelin sheath per axon compared to control groups, suggesting that ABEs properly correct mutant adenine and restores myelination. (Figure 15)

In contrast, when observing structure of myelin in sciatic nerve, no significant difference was found among all groups. As a result of counting the number of myelinated axons in the same range of field, there was also no significant difference between ABE treated groups and control group. (Figure 16) Judging from the above experimental results, ABE8e and ABE8eWQ recovered myelin sheath in the central nervous system, but failed to recover myelin sheath in the peripheral nervous system

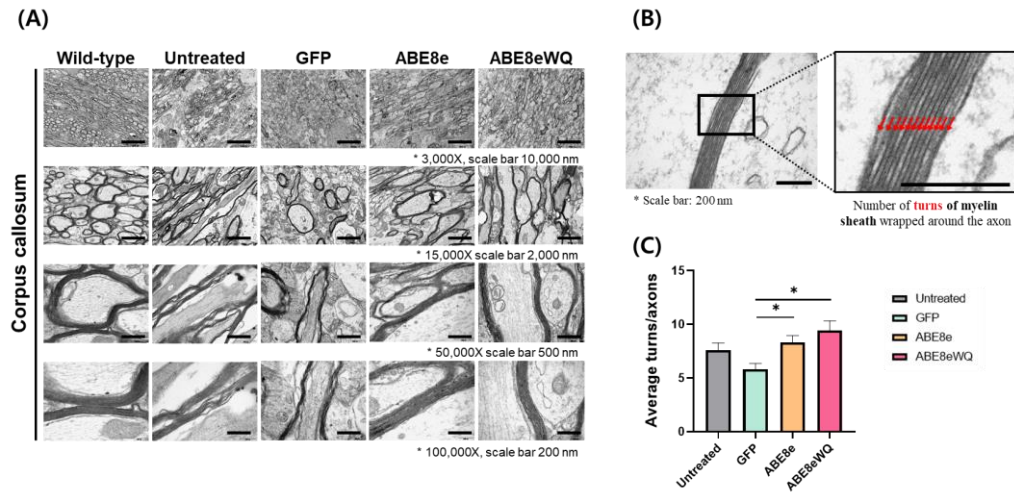


**Figure 15. Transmission electron microscopy (TEM) images of corpus callosum.** (A) Images represent myelination of the corpus callosum in each group. (B, C) The average number of turns of myelin sheath around the axons was counted. Data were analyzed using the one-way ANOVA and post-hoc comparisons (Bonferroni). (Number of experimental samples; Untreated:  $n = 10$  from two mice, GFP:  $n = 15$  from three mice, ABE8e  $n = 10$  from two mice, ABE8eWQ:  $n = 5$  from one mouse) The data are presented as mean  $\pm$  SEM. \* $p < 0.05$ , \*\* $p < 0.01$ , \*\*\* $p < 0.001$ . ABE: adenine base editor, GFP: green fluorescent protein. Scale bar: 200 nm. Scale bar for 3,000X images: 10,000 nm; scale bar for 15,000X images: 2,000 nm; scale bar for 50,000X images: 500 nm, scale bar for 100,000X images: 200 nm.

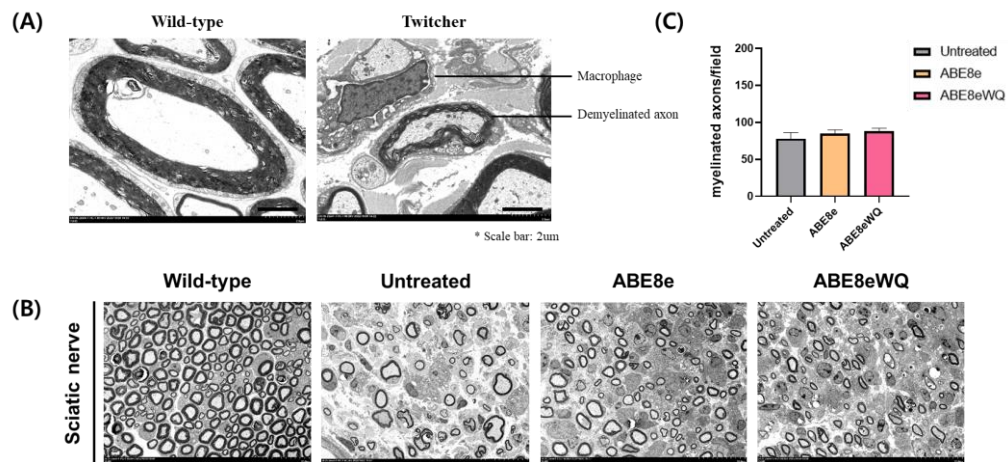


**Figure 16. Transmission electron microscopy (TEM) images of sciatic nerve.** (A) Myelinated axons in the sciatic nerve of twitcher showed demyelination and macrophage infiltration unlike wild-type mouse. Scale bar: 2 μm. (B) Images represents myelination of the sciatic nerve in each group. (C) The number of myelinated axons was counted. No significant differences were observed. (Number of experimental samples; Untreated: n = 5 from one mouse, ABE8e n = 10 from two mice, ABE8eWQ: n = 5 from one mouse) Data were analyzed using the one-way ANOVA and post-hoc comparisons (Bonferroni). The data are presented as mean ± SEM. \* $p < 0.05$ , \*\* $p < 0.01$ , \*\*\* $p < 0.001$ . ABE: adenine base editor, EM: electron microscopy.

**Table 15. Heterogeneity of variance information of TEM image analysis**

Region	Parameter (Numbers)	Untreated	GFP	ABE8e	ABE8eWQ	F-value	P-value
Corpus callosum	Average turns of myelin	7.6 ± 0.7	5.8 ± 0.6	8.3 ± 0.7	9.4 ± 0.9	4.876	0.006
Sciatic nerve	Myelinated axons	78.0 ± 8.4	-	84.8 ± 5.3	88.2 ± 4.0	0.550	0.587

Note : Data are presented as mean ± SEM. Statistical analysis were conducted using the one-way ANOVA and post-hoc comparisons (Bonferroni). TEM: transmission electron microscopy, ABE: adenine base editor, GFP: green fluorescent protein.

**Table 16. Statistical information of TEM image analysis**

	Comparison regions			N		<i>P</i> -value
Average turns of myelin in corpus callosum	Untreated	vs.	GFP	10 : 15	ns	0.277
		vs.	ABE8e	10 : 10	ns	1.000
		vs.	ABE8eWQ	10 : 5	ns	0.795
	GFP	vs.	ABE8e	15 : 10	*	0.041
		vs.	ABE8eWQ	15 : 5	*	0.014
		vs.	ABE8eWQ	10 : 5	ns	1.000
Myelinated axons in sciatic nerve	Untreated	vs.	ABE8e	5 : 10	ns	1.000
		vs.	ABE8eWQ	5 : 5	ns	0.964
	ABE8e	vs.	ABE8eWQ	10 : 5	ns	1.000

Note : Data are presented as mean  $\pm$  SEM. Statistical analysis were conducted using the one-way ANOVA and post-hoc comparisons (Bonferroni). \* $p < 0.05$ , \*\* $p < 0.01$ , \*\*\* $p < 0.001$ , ns: non-significance. ABE: adenine base editor, GFP: green fluorescent protein.

## 8. Both ABE8e and ABE8eWQ increased myelin integrity and decreased the number of PAS-positive cells

To confirm the myelin sheaths integrity and the macrophage infiltration status, LFB/PAS stain was conducted with corpus callosum, cerebellum and spinal cord of all groups. The untreated twitcher mouse is characterized by infiltration of PAS-positive foamy macrophages consistent with myelin loss in these histological sites. In ABE treated groups, however, the blue staining of intact myelin was stronger and the layer of myelin sheaths in the corpus callosum was thicker. Even if the thickness of the corpus callosum increased after ABE treatment, it was hard to be told that it is completely normal looking as wild-type group and statistically significant difference was not shown. (Figure 17)

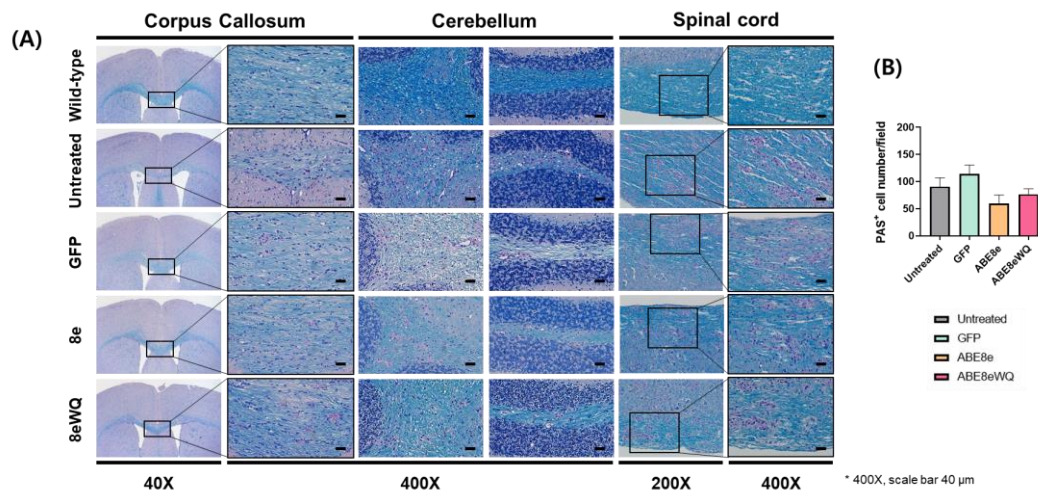


**Figure 17. LFB/PAS staining analysis on remyelination following ABE treatment.** (A) LFB/PAS staining images in corpus callosum, cerebellum and spinal cord. LFB (blue) stains myelin and PAS (pink) stains globoid cells. Scale bar: 40  $\mu$ m. (B) PAS-positive cell number was counted in 40X images of corpus callosum. (Untreated: n = 8, GFP: n = 5, ABE8e n = 4, ABE8eWQ: n = 4) Data were analyzed using the one-way ANOVA and post-hoc comparisons (Bonferroni). The data are presented as mean  $\pm$  SEM. ABE: adenine base editor, GFP: green fluorescent protein.

**Table 17. Heterogeneity of variance information of the number of PAS positive cells**

	<b>Untreated</b>	<b>GFP</b>	<b>ABE8e</b>	<b>ABE8eWQ</b>	<b>F-value</b>	<b>P-value</b>
PAS positive cells (Numbers / field)	8.1 ± 0.7	8.3 ± 1.1	6.2 ± 1.0	6.1 ± 1.3	1.406	0.275

Note : Data are presented as mean ± SEM. Statistical analysis were conducted using the one-way ANOVA and post-hoc comparisons (Bonferroni). PAS: Periodic acid–Schiff, ABE: adenine base editor, GFP: green fluorescent protein.

**Table 18. Statistical information of the number of PAS positive cells**

		Comparison regions		N		P-value
PAS positive cells	Untreated	vs.	GFP	8 : 5	ns	1.000
		vs.	ABE8e	8 : 4	ns	0.885
		vs.	ABE8eWQ	8 : 4	ns	1.000
	GFP	vs.	ABE8e	5 : 4	ns	0.943
		vs.	ABE8eWQ	5 : 4	ns	1.000
		vs.	ABE8eWQ	4 : 4	ns	1.000

Note : Data are presented as mean  $\pm$  SEM. Statistical analysis were conducted using the one-way ANOVA and post-hoc comparisons (Bonferroni). \* $p < 0.05$ , \*\* $p < 0.01$ , \*\*\* $p < 0.001$ , ns: non-significance. ABE: adenine base editor, GFP: green fluorescent protein.

### **9. Both ABE8e and ABE8eWQ induced white matter recovery in the diffusion tensor images of brain MRI**

MRI was conducted on P38, just before sacrifice. Several types of DTI (Diffusion Tensor Imaging) were used to evaluate the structural integrity of the white matter fiber tract. Fractional anisotropy (FA) and axial diffusivity (AD) of ABE treated group were remarkably brighter than those of control groups in the corpus callosum. Otherwise, mean diffusivity (MD) and radial diffusivity (RD) of ABE treated group were remarkably darker than those of untreated and GFP group in the corpus callosum (Figure 18). All things considered, evaluating the level of remyelination using various experimental tools, it was confirmed that treatment of ABE8e and ABE8eWQ had similar therapeutic effects.

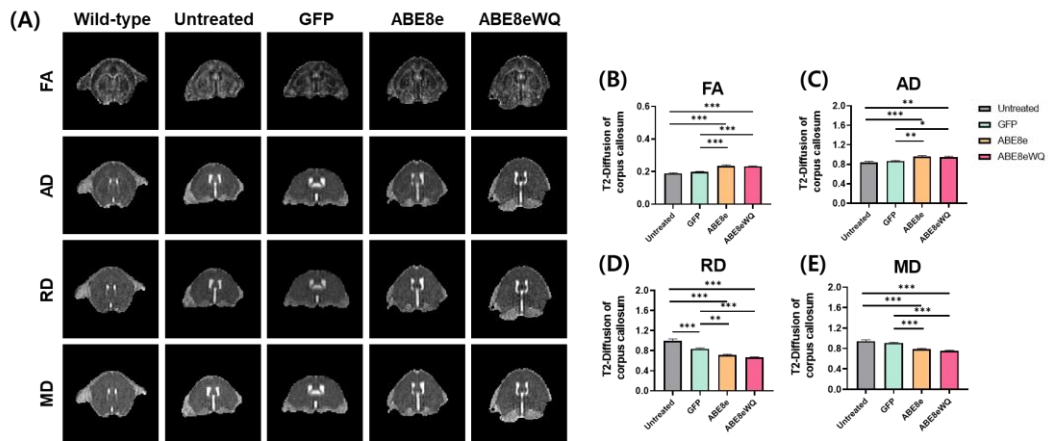


**Figure 18. Diffusion tensor imaging (DTI) analysis of the brain.** DTI parameters on P38. The representative images of each parameter (A) have been considered for the analysis of white matter degeneration through FA (B), AD (C), RD (D) and MD (E). (Number of experimental samples from four mice; Untreated: n = 16, GFP: n = 16, ABE8e n = 16, ABE8eWQ: n = 16) Data were analyzed using the one-way ANOVA and post-hoc comparisons (Bonferroni). The data are presented as mean  $\pm$  SEM. \* $p < 0.05$ , \*\* $p < 0.01$ , \*\*\* $p < 0.001$ . ABE: adenine base editor, GFP: green fluorescent protein, FA: fractional anisotropy, AD: axial diffusivity, RD: radial diffusivity, MD: mean diffusivity.

**Table 19. Heterogeneity of variance information of DTI parameters in the corpus callosum**

<b>Region</b>	<b>DTI</b>	<b>Untreated</b>	<b>GFP</b>	<b>ABE8e</b>	<b>ABE8eWQ</b>	<b>F-value</b>	<b>P-value</b>
Corpus callosum	FA	0.19 ± 0.00	0.20 ± 0.00	0.23 ± 0.01	0.23 ± 0.00	21.217	< 0.001
	AD	0.84 ± 0.02	0.87 ± 0.01	0.96 ± 0.02	0.94 ± 0.02	9.199	< 0.001
	RD	0.99 ± 0.04	0.84 ± 0.02	0.71 ± 0.02	0.67 ± 0.01	39.384	< 0.001
	MD	0.94 ± 0.03	0.91 ± 0.01	0.79 ± 0.02	0.76 ± 0.01	26.187	< 0.001

Note : Data are presented as mean ± SEM. Statistical analysis were conducted using the one-way ANOVA and post-hoc comparisons (Bonferroni). DTI: diffusion tensor imaging, FA: fractional anisotropy, AD: axial diffusivity, RD: radial diffusivity, MD: mean diffusivity, ABE: *adenine base* editor, GFP: green fluorescent protein.

**Table 20. Heterogeneity of variance information of DTI parameters in the corpus callosum**

Region	DTI	Comparison groups		N	P-value	
Corpus callosum	FA	Untreated	vs. GFP	16 : 16	ns	1.000
			vs. ABE8e	16 : 16	***	0.000
		GFP	vs. ABE8eWQ	16 : 16	***	0.000
			vs. ABE8e	16 : 16	***	0.000
		ABE8e	vs. ABE8eWQ	16 : 16	***	0.000
			vs. ABE8eWQ	16 : 16	ns	1.000
	AD	Untreated	vs. GFP	16 : 16	ns	1.000
			vs. ABE8e	16 : 16	***	0.000
		GFP	vs. ABE8eWQ	16 : 16	**	0.002
			vs. ABE8e	16 : 16	**	0.008
		ABE8e	vs. ABE8eWQ	16 : 16	*	0.046
			vs. ABE8eWQ	16 : 16	ns	1.000
	RD	Untreated	vs. GFP	16 : 16	***	0.000
			vs. ABE8e	16 : 16	***	0.000
		GFP	vs. ABE8eWQ	16 : 16	***	0.000
			vs. ABE8e	16 : 16	**	0.002
		ABE8e	vs. ABE8eWQ	16 : 16	***	0.000
			vs. ABE8eWQ	16 : 16	ns	1.000
	MD	Untreated	vs. GFP	16 : 16	ns	1.000
			vs. ABE8e	16 : 16	***	0.000
		GFP	vs. ABE8eWQ	16 : 16	***	0.000
			vs. ABE8e	16 : 16	***	0.000
		ABE8e	vs. ABE8eWQ	16 : 16	***	0.000
			vs. ABE8eWQ	16 : 16	ns	1.000

Note : Data are presented as mean  $\pm$  SEM. Statistical analysis were conducted using the one-way ANOVA and post-hoc comparisons (Bonferroni). \* $p$  < 0.05, \*\* $p$  < 0.01, \*\*\* $p$  < 0.001 or ns: non-significance. DTI: diffusion tensor imaging, FA: fractional anisotropy, AD: axial diffusivity, RD: radial diffusivity, MD: mean diffusivity, ABE: *adenine base editor*, GFP: green fluorescent protein.

## 10. Low mRNA expression of split ABEs and gene editing efficiency were shown in heart, liver, spinal cord and sciatic nerve

To determine if the injected materials has spread to internal organs, we selected four specific internal organs as follows: heart, liver, spinal cord and sciatic nerve. Since the injection was performed directly into the mouse brain using same AAV9 vector, the mRNA of both ABE –NT and CT was hardly distributed to internal organs. (Figure 19) And editing efficiency of mutant adenine ( $A_5$ ) in organs was also obviously lower than that in mouse brain. (Figure 20)

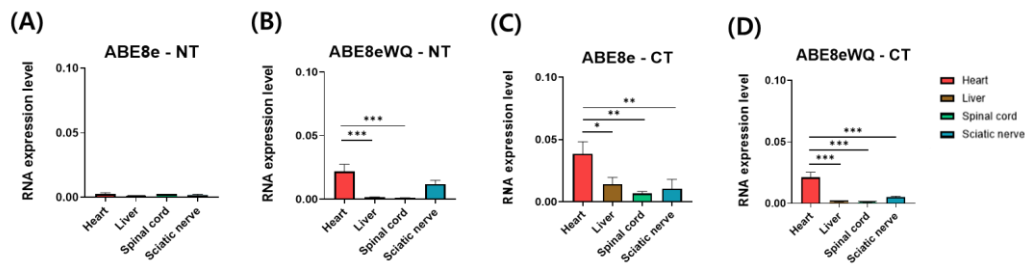


**Figure 19. RNA expression levels of viral vectors in heart, liver, spinal cord and sciatic nerve.** The mRNA expression levels show distribution of AAV9 viral vectors *in vivo*. N-terminal (A) and C-terminal (C) of ABE8e, and N-terminal (B) and C-terminal (D) of ABE8eWQ were shown. (Number of experimental samples from four mice; Untreated: n = 12, GFP: n = 12, ABE8e n = 12, ABE8eWQ: n = 12) The experimental samples were extracted from four internal organs: heart, liver, spinal cord and sciatic nerve. Data were analyzed using the one-way ANOVA and post-hoc comparisons (Bonferroni). The data are presented as mean  $\pm$  SEM. \* $p < 0.05$ , \*\* $p < 0.01$ , \*\*\* $p < 0.001$ . ABE: adenine base editor.

**Table 21. Heterogeneity of variance information of mRNA expression in heart, liver, spinal cord and sciatic nerve**

<b>Region</b>	<b>ABE8e - NT</b>	<b>ABE8e - CT</b>	<b>ABE8eWQ - NT</b>	<b>ABE8eWQ - CT</b>
Heart	0.0026 ± 0.0010	0.0386 ± 0.0097	0.0218 ± 0.0056	0.0211 ± 0.0043
Liver	0.0005 ± 0.0002	0.0142 ± 0.0053	0.0014 ± 0.0004	0.0011 ± 0.0002
Spinal cord	0.0013 ± 0.0004	0.0067 ± 0.0017	0.0010 ± 0.0002	0.0008 ± 0.0001
Sciatic nerve	0.0019 ± 0.0005	0.0036 ± 0.0018	0.0120 ± 0.0028	0.0052 ± 0.0006
<b>F-value</b>	2.052	6.720	9.885	19.658
<b>P-value</b>	0.126	0.001	< 0.001	< 0.001

Note : Data are presented as mean ± SEM. Statistical analysis were conducted using the one-way ANOVA and post-hoc comparisons (Bonferroni). ABE: adenine base editor, FC: frontal cortex, CC: corpus callosum, HC: hippocampus, CB: cerebellum.

**Table 22. Statistical information of mRNA expression in heart, liver, spinal cord and sciatic nerve**

<b>Split ABEs</b>	<b>Comparison regions</b>			<b>N</b>	<b>P-value</b>	
ABE8e - NT	Heart	vs.	Liver	9 : 9	ns	0.142
		vs.	Spinal cord	9 : 9	ns	0.864
		vs.	Sciatic nerve	9 : 9	ns	1.000
	Liver	vs.	Spinal cord	9 : 9	ns	1.000
		vs.	Sciatic nerve	9 : 9	ns	0.728
		Spinal cord	vs.	Sciatic nerve	9 : 9	ns
ABE8e -CT	Heart	vs.	Liver	9 : 9	*	0.040
		vs.	Spinal cord	9 : 9	**	0.004
		vs.	Sciatic nerve	9 : 6	**	0.005
	Liver	vs.	Spinal cord	9 : 9	ns	1.000
		vs.	Sciatic nerve	9 : 6	ns	1.000
		Spinal cord	vs.	Sciatic nerve	9 : 6	ns
ABE8eWQ -NT	Heart	vs.	Liver	9 : 9	***	0.000
		vs.	Spinal cord	9 : 9	***	0.000
		vs.	Sciatic nerve	9 : 9	ns	0.214
	Liver	vs.	Spinal cord	9 : 9	ns	1.000
		vs.	Sciatic nerve	9 : 9	ns	0.138
		Spinal cord	vs.	Sciatic nerve	9 : 9	ns
ABE8eWQ -CT	Heart	vs.	Liver	9 : 9	***	0.000
		vs.	Spinal cord	9 : 9	***	0.000
		vs.	Sciatic nerve	9 : 9	***	0.000
	Liver	vs.	Spinal cord	9 : 9	ns	1.000
		vs.	Sciatic nerve	9 : 9	ns	1.000
		Spinal cord	vs.	Sciatic nerve	9 : 9	ns

Note : Data are presented as mean  $\pm$  SEM. Statistical analysis were conducted using the one-way ANOVA and post-hoc comparisons (Bonferroni). \* $p < 0.05$ , \*\* $p < 0.01$ , \*\*\* $p < 0.001$ , ns: non-significance. ABE: adenine base editor, FC: frontal cortex, CC: corpus callosum, HC: hippocampus, CB: cerebellum.

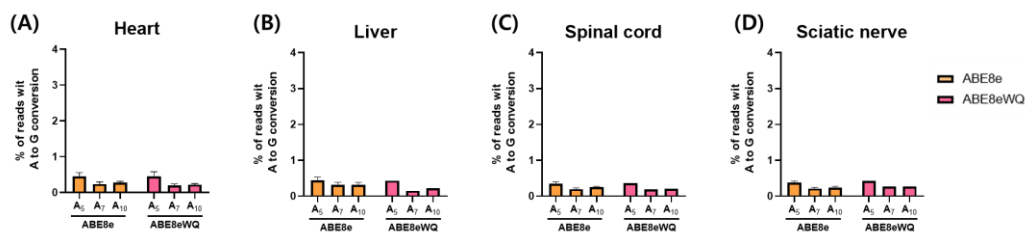


**Figure 20. Gene editing efficiency of ABE8e and ABE8eWQ in heart, liver, spinal cord and sciatic nerve.** Percentage of adenine conversion for evaluating the efficiencies and outcomes of base editing. Graphs show the base substitution activity of each ABE on A5 (A) which is a target adenine, A7 (B) and A10 (C) which are bystanders. (ABE8e n = 3, ABE8eWQ: n = 3) No significant differences were observed. The experimental samples were extracted from four internal organs: heart, liver, spinal cord and sciatic nerve. ABE: adenine base editor.

**Table 23. Heterogeneity of variance information of mRNA expression in heart, liver, spinal cord and sciatic nerve**

		Heart	Liver	Spinal cord	Sciatic nerve
ABE8e	A <sub>5</sub>	0.453 ± 0.103	0.513 ± 0.092	0.347 ± 0.041	0.423 ± 0.035
	A <sub>7</sub>	0.237 ± 0.063	0.420 ± 0.035	0.223 ± 0.035	0.263 ± 0.007
	A <sub>10</sub>	0.277 ± 0.038	0.347 ± 0.107	0.247 ± 0.020	0.257 ± 0.054
	F-value	2.477	0.986	3.863	6.411
	P-value	0.164	0.426	0.084	0.032
ABE8eWQ	A <sub>5</sub>	0.450 ± 0.130	0.373 ± 0.099	0.343 ± 0.101	0.340 ± 0.053
	A <sub>7</sub>	0.203 ± 0.038	0.157 ± 0.035	0.163 ± 0.037	0.177 ± 0.042
	A <sub>10</sub>	0.223 ± 0.027	0.247 ± 0.048	0.227 ± 0.048	0.230 ± 0.023
	F-value	2.945	2.653	1.791	4.098
	P-value	0.129	0.149	0.246	0.075

Note : Data are presented as mean ± SEM. Statistical analysis were conducted using the one-way ANOVA and post-hoc comparisons (Bonferroni). ABE: adenine base editor, FC: frontal cortex, CC: corpus callosum, HC: hippocampus, CB: cerebellum.

**Table 24. Statistical information of mRNA expression in heart, liver, spinal cord and sciatic nerve**

Region		Comparison regions			N		P-value
Heart	ABE8e	A <sub>5</sub>	vs.	A <sub>7</sub>	3 : 3	ns	0.244
			vs.	A <sub>10</sub>	3 : 3	ns	0.417
	ABE8eWQ	A <sub>7</sub>	vs.	A <sub>10</sub>	3 : 3	ns	1.000
		A <sub>5</sub>	vs.	A <sub>7</sub>	3 : 3	ns	0.215
			vs.	A <sub>10</sub>	3 : 3	ns	0.274
		A <sub>7</sub>	vs.	A <sub>10</sub>	3 : 3	ns	1.000
Liver	ABE8e	A <sub>5</sub>	vs.	A <sub>7</sub>	3 : 3	ns	1.000
			vs.	A <sub>10</sub>	3 : 3	ns	0.632
	ABE8eWQ	A <sub>7</sub>	vs.	A <sub>10</sub>	3 : 3	ns	1.000
		A <sub>5</sub>	vs.	A <sub>7</sub>	3 : 3	ns	0.185
			vs.	A <sub>10</sub>	3 : 3	ns	0.686
		A <sub>7</sub>	vs.	A <sub>10</sub>	3 : 3	ns	1.000
Spinal cord	ABE8e	A <sub>5</sub>	vs.	A <sub>7</sub>	3 : 3	ns	0.119
			vs.	A <sub>10</sub>	3 : 3	ns	0.234
	ABE8eWQ	A <sub>7</sub>	vs.	A <sub>10</sub>	3 : 3	ns	1.000
		A <sub>5</sub>	vs.	A <sub>7</sub>	3 : 3	ns	0.334
			vs.	A <sub>10</sub>	3 : 3	ns	0.816
		A <sub>7</sub>	vs.	A <sub>10</sub>	3 : 3	ns	1.000
Sciatic nerve	ABE8e	A <sub>5</sub>	vs.	A <sub>7</sub>	3 : 3	ns	0.069
			vs.	A <sub>10</sub>	3 : 3	ns	0.059
	ABE8eWQ	A <sub>7</sub>	vs.	A <sub>10</sub>	3 : 3	ns	1.000
		A <sub>5</sub>	vs.	A <sub>7</sub>	3 : 3	ns	0.093
			vs.	A <sub>10</sub>	3 : 3	ns	0.323
		A <sub>7</sub>	vs.	A <sub>10</sub>	3 : 3	ns	1.000

Note : Data are presented as mean  $\pm$  SEM. Statistical analysis were conducted using the one-way ANOVA and post-hoc comparisons (Bonferroni). \* $p$  < 0.05, \*\* $p$  < 0.01, \*\*\* $p$  < 0.001, ns: non-significance.

### 11. Tumor or dysplasia was not identified in brain, heart, liver and spinal cord after ABE treatments

Histological comparison between control groups and ABE treated groups was conducted to prove the safety of ABE treatment. Images were used after hematoxylin and eosin staining to confirm that all treatments used in the study did not have tumorigenicity. Fortunately, no pathological phenomena were found both in brain and in internal organs. (Figure 21, 22)

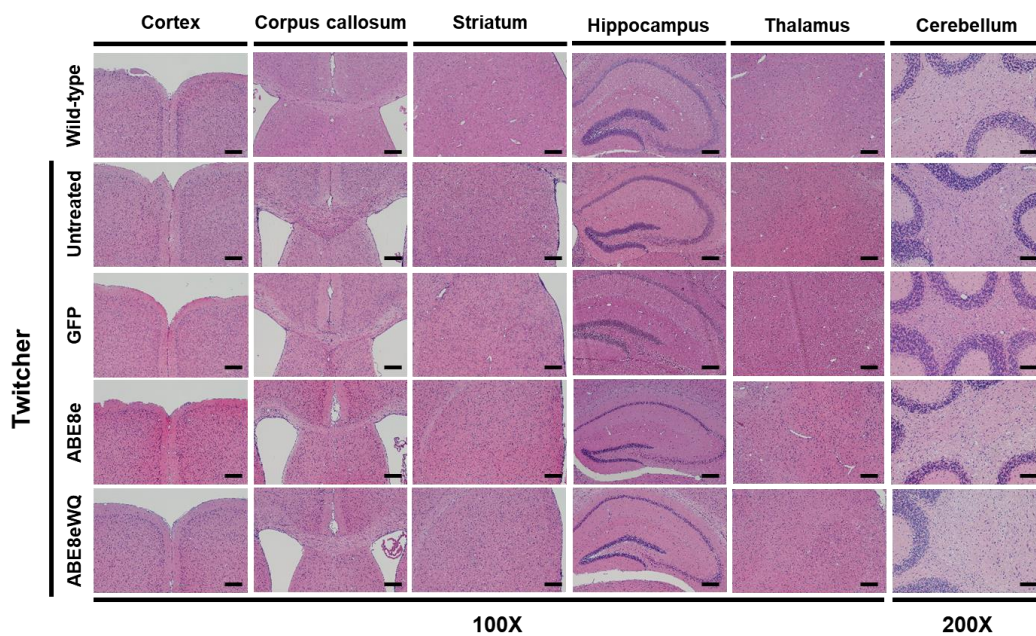


**Figure 21. Hematoxylin and eosin staining of six brain regions.** Hematoxylin and eosin staining of brain tissue. 4  $\mu\text{m}$  thick mouse brain slices were used. Images of cortex, corpus callosum, striatum, hippocampus and thalamus were magnified a hundredfold, while those of cerebellum were magnified two hundred times. Scale bar for 100X images: 200  $\mu\text{m}$ , scale bar for 200X images: 100  $\mu\text{m}$ .

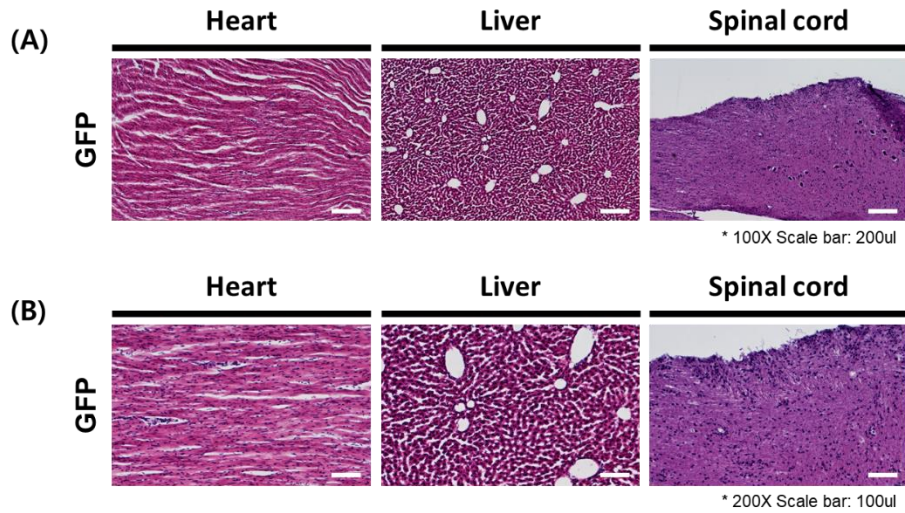


**Figure 22. Hematoxylin and eosin staining of heart, liver and spinal cord.** Hematoxylin and eosin staining of three internal organs. 4  $\mu\text{m}$  thick mouse organ slices were used. (A) Images were magnified a hundredfold. Scale bar: 200  $\mu\text{m}$ . (B) Images were magnified two hundred times. Scale bar: 100  $\mu\text{m}$ .

## 12. ABE treatments to wild-type mice produced no statistical difference in all behavioral assessments

To confirm the safety of our treatment material, ABE8e and ABE8eWQ were injected into wild type mice and the progress was observed. Krabbe disease was believed to have autosomal recessive pattern, suggesting heterozygous carrier mice did not show the behavioral deficits.<sup>19</sup> But we tested only with homozygous wild-type mice.

With young wild-type mice, the body weight was measured and all behavioral tests were conducted three times on P21, P28 and P35. Statistical analysis was conducted using both one-way ANOVA and two-way ANOVA. Here, no significant differences were found in body weight of all groups. (Figure 23) And the results of the clasping test and three types of rotarod tests also have no significant difference between control groups and ABE treated groups. (Figure 24, 25)

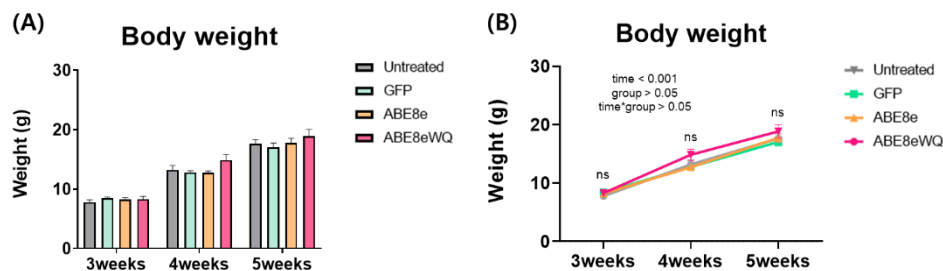


**Figure 23. Body weights in ABE treated wild-type mouse groups.** The measurement of body weight. (Untreated: n = 11, GFP: n = 11, ABE8e n = 9, ABE8eWQ: n = 11) No significant differences were observed. The data are presented as mean  $\pm$  SEM. The statistics used for the bar graph (A) were the one-way ANOVA (Bonferroni), whereas the statistics used for the line graph (B) were two-way ANOVA which is used to estimate how the mean of a quantitative variable changes according to the levels of two categorical variables, the time and disease conditions. \* $p < 0.05$ , \*\* $p < 0.01$ , \*\*\* $p < 0.001$ . ABE: adenine base editor, GFP: green fluorescent protein.

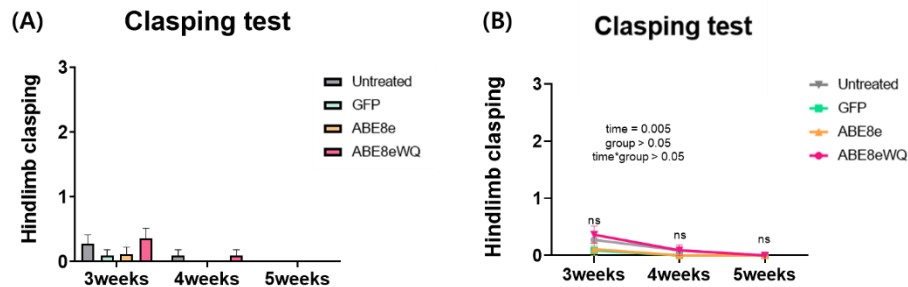


**Figure 24. Clasp test in ABE treated wild-type mouse groups.** Duration time of limb clasping under 10 seconds of tail-suspension was monitored. (Untreated: n = 11, GFP: n = 11, ABE8e n = 9, ABE8eWQ: n = 11) No significant differences were observed. The data are presented as mean  $\pm$  SEM. The statistics used for the bar graph (A) were the one-way ANOVA (Bonferroni), whereas the statistics used for the line graph (B) were two-way ANOVA which is used to estimate how the mean of a quantitative variable changes according to the levels of two categorical variables, the time and disease conditions. \* $p < 0.05$ , \*\* $p < 0.01$ , \*\*\* $p < 0.001$ . ABE: adenine base editor, GFP: green fluorescent protein.

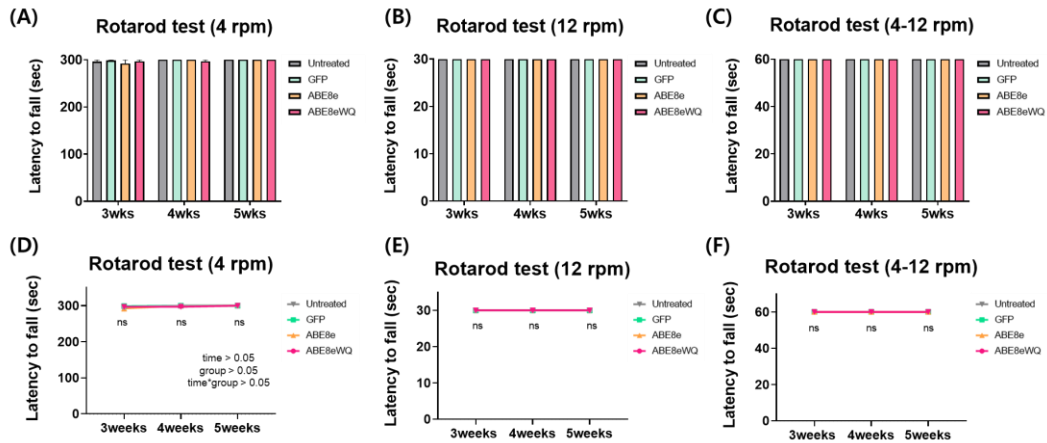


**Figure 25. Rotarod scores in ABE treated wild-type mouse groups.** Mice were tested at three different kinds of speeds in a rotarod apparatus; constant speed of 4 rpm (A, D) and 12 rpm (B, E), and accelerating speed of 4 to 40 rpm (C, F). The latency time to fall from the rolling rod within 5 min was recorded. (Untreated: n = 40, GFP: n = 40, ABE8e n = 20, ABE8eWQ: n = 21) No significant differences were observed. The data are presented as mean  $\pm$  SEM. The statistics used for the bar graph were the one-way ANOVA (Bonferroni), whereas the statistics used for the line graph were two-way ANOVA which is used to estimate how the mean of a quantitative variable changes according to the levels of two categorical variables, the time and disease conditions. \* $p < 0.05$ , \*\* $p < 0.01$ , \*\*\* $p < 0.001$ . ABE: adenine base editor, GFP: green fluorescent protein.

**Table 25. Heterogeneity of variance information of the behavioral assessment in wild-type mice**

Test	Week	Untreated	GFP	ABE8e	ABE8eWQ	F-value	P-value
Body weight	3	7.8 ± 0.4	8.4 ± 0.2	8.2 ± 0.3	8.3 ± 0.5	0.636	0.597
	4	13.2 ± 0.8	12.8 ± 0.3	12.7 ± 0.3	14.8 ± 1.0	2.195	0.105
	5	17.6 ± 0.7	17.0 ± 0.7	17.7 ± 0.8	18.8 ± 1.2	0.766	0.520
Clasping	3	0.3 ± 0.1	0.1 ± 0.1	0.1 ± 0.1	0.4 ± 0.2	1.060	0.377
	4	0.1 ± 0.1	0.0 ± 0.0	0.0 ± 0.0	0.1 ± 0.1	0.603	0.617
	5	0.0 ± 0.0	0.0 ± 0.0	0.0 ± 0.0	0.0 ± 0.0	-	-
Rotarod constant (4 rpm)	3	296 ± 3.6	299 ± 1.5	292 ± 7.7	297 ± 3.3	0.354	0.786
	4	300 ± 0.0	300 ± 0.0	300 ± 0.0	297 ± 3.3	0.935	0.433
	5	300 ± 0.0	300 ± 0.0	300 ± 0.0	300 ± 0.0	-	-
Rotarod constant (12 rpm)	3	30.0 ± 0.0	30.0 ± 0.0	30.0 ± 0.0	30.0 ± 0.0	-	-
	4	30.0 ± 0.0	30.0 ± 0.0	30.0 ± 0.0	30.0 ± 0.0	-	-
	5	30.0 ± 0.0	30.0 ± 0.0	30.0 ± 0.0	30.0 ± 0.0	-	-
Rotarod accelerated (4-12 rpm)	3	60.0 ± 0.0	60.0 ± 0.0	60.0 ± 0.0	60.0 ± 0.0	-	-
	4	60.0 ± 0.0	60.0 ± 0.0	60.0 ± 0.0	60.0 ± 0.0	-	-
	5	60.0 ± 0.0	60.0 ± 0.0	60.0 ± 0.0	60.0 ± 0.0	-	-

Note : Data are presented as mean ± SEM. Statistical analysis were conducted using the one-way ANOVA and post-hoc comparisons (Bonferroni). ABE: adenine base editor, GFP: green fluorescent protein.

**Table 26. Statistical information of the behavioral assessment in wild-type mice**

		Comparison regions		N	P-value	
Body weight	Untreated	vs.	GFP	11 : 11	ns	1.000
		vs.	ABE8e	11 : 9	ns	1.000
		vs.	ABE8eWQ	11 : 11	ns	1.000
	GFP	vs.	ABE8e	11 : 9	ns	1.000
		vs.	ABE8eWQ	11 : 11	ns	0.875
		ABE8e	vs.	ABE8eWQ	9 : 11	ns
Clasping	Untreated	vs.	GFP	11 : 11	ns	1.000
		vs.	ABE8e	11 : 9	ns	1.000
		vs.	ABE8eWQ	11 : 11	ns	1.000
	GFP	vs.	ABE8e	11 : 9	ns	1.000
		vs.	ABE8eWQ	11 : 11	ns	1.000
		ABE8e	vs.	ABE8eWQ	9 : 11	ns
Rotarod constant (4 rpm)	Untreated	vs.	GFP	11 : 11	ns	1.000
		vs.	ABE8e	11 : 9	ns	1.000
		vs.	ABE8eWQ	11 : 11	ns	1.000
	GFP	vs.	ABE8e	11 : 9	ns	1.000
		vs.	ABE8eWQ	11 : 11	ns	1.000
		ABE8e	vs.	ABE8eWQ	9 : 11	ns
Rotarod constant (12 rpm)	Untreated	vs.	GFP	11 : 11	ns	-
		vs.	ABE8e	11 : 9	ns	-
		vs.	ABE8eWQ	11 : 11	ns	-
	GFP	vs.	ABE8e	11 : 9	ns	-
		vs.	ABE8eWQ	11 : 11	ns	-

	ABE8e	vs.	ABE8eWQ	9 : 11	ns	-
	Untreated	vs.	GFP	11 : 11	ns	-
Rotarod accelerated (4-12 rpm)		vs.	ABE8e	11 : 9	ns	-
		vs.	ABE8eWQ	11 : 11	ns	-
	GFP	vs.	ABE8e	11 : 9	ns	-
		vs.	ABE8eWQ	11 : 11	ns	-
	ABE8e	vs.	ABE8eWQ	9 : 11	ns	-

Note : Data are presented as mean  $\pm$  SEM. Statistical analysis were conducted using the one-way ANOVA and post-hoc comparisons (Bonferroni). \* $p < 0.05$ , \*\* $p < 0.01$ , \*\*\* $p < 0.001$  or ns: non-significance. ABE: adenine base editor, GFP: green fluorescent protein.

### 13. ABE treated wild-type mice showed no behavioral abnormalities despite aging corpus callosum

Same experiments were conducted with old wild-type mice (P450-700). With these mice, the body weight measurement and behavioral test was conducted at once. No significant differences were observed here as well as young wild-type mice (P21-35). (Figure 26) In other words, any side effects or clinical abnormalities caused by AAV vector injection were not found. Treatment of ABE8e and ABE8eWQ did not disrupted the normal phenotype of wild-type mice.

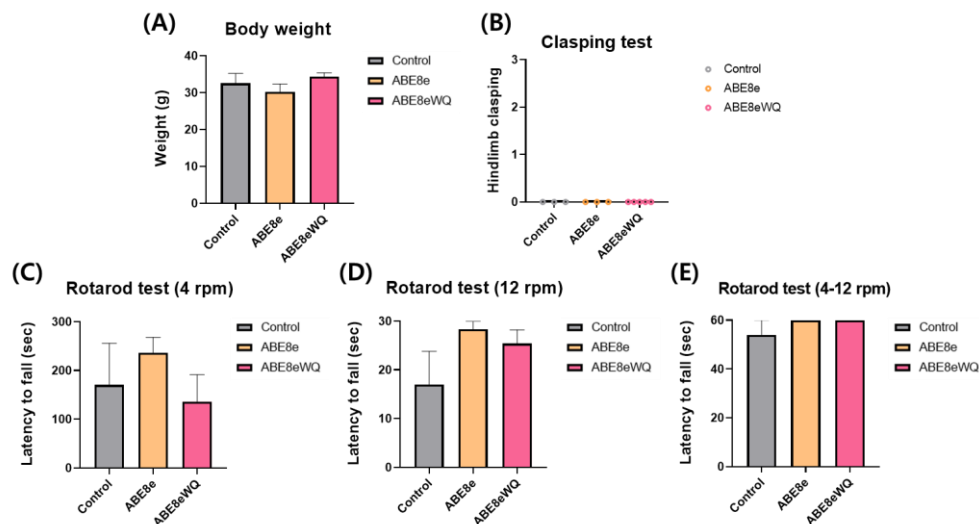


**Figure 26. Behavioral assessments in ABE-treated wild-type old mice.** Behavioral tests were conducted using ABE-treated old mice (450-700 days) to prove the safety of ABE8e and ABE8eWQ (Control: n = 3, ABE8e: n = 3, ABE8eWQ n = 5). (A) The body weight was measured. (B) Duration time of limb clasping under 10 seconds of tail-suspension was monitored. Finally, mice were tested at three different kinds of speeds in a rotarod apparatus; constant speed of 4 rpm (C) and 12 rpm (D), and accelerating speed of 4 to 40 rpm (E). No significant differences were observed. Data were analyzed using the one-way ANOVA and post-hoc comparisons (Bonferroni). The data are presented as mean  $\pm$  SEM. ABE: adenine base editor.

**Table 27. Heterogeneity of variance information of the behavioral assessment in old wild-type mice**

Test	Control	ABE8e	ABE8eWQ	<i>F</i> -value	<i>P</i> -value
Body weight	32.5 ± 2.6	30.2 ± 2.2	34.4 ± 1.0	1.453	0.290
Clasping	0.0 ± 0.0	0.0 ± 0.0	0.0 ± 0.0	-	-
Rotarod constant (4 rpm)	170 ± 85.5	236 ± 31.9	136 ± 55.5	0.677	0.535
Rotarod constant (12 rpm)	17.0 ± 6.8	28.3 ± 1.7	25.4 ± 2.8	1.878	0.215
Rotarod accelerated (4-12 rpm)	52.0 ± 8.0	60.0 ± 0.0	60.0 ± 0.0	1.455	0.289

Note : Data are presented as mean ± SEM. Statistical analysis were conducted using the one-way ANOVA and post-hoc comparisons (Bonferroni). ABE: adenine base editor, GFP: green fluorescent protein.

**Table 28. Statistical information of the behavioral assessment in old wild-type mice**

		Comparison regions		N	P-value	
Body weight	Control	vs.	ABE8e	3 : 3	ns	1.000
		vs.	ABE8eWQ	3 : 5	ns	1.000
	ABE8e	vs.	ABE8eWQ	3 : 5	ns	0.382
Clasping	Control	vs.	ABE8e	3 : 3	ns	-
		vs.	ABE8eWQ	3 : 5	ns	-
	ABE8e	vs.	ABE8eWQ	3 : 5	ns	-
Rotarod constant (4 rpm)	Control	vs.	ABE8e	3 : 3	ns	1.000
		vs.	ABE8eWQ	3 : 5	ns	1.000
	ABE8e	vs.	ABE8eWQ	3 : 5	ns	0.835
Rotarod constant (12 rpm)	Control	vs.	ABE8e	3 : 3	ns	0.308
		vs.	ABE8eWQ	3 : 5	ns	0.496
	ABE8e	vs.	ABE8eWQ	3 : 5	ns	1.000
Rotarod accelerated (4-12 rpm)	Control	vs.	ABE8e	3 : 3	ns	0.585
		vs.	ABE8eWQ	3 : 5	ns	0.458
	ABE8e	vs.	ABE8eWQ	3 : 5	ns	1.000

Note : Data are presented as mean  $\pm$  SEM. Statistical analysis were conducted using the one-way ANOVA and post-hoc comparisons (Bonferroni). \* $p < 0.05$ , \*\* $p < 0.01$ , \*\*\* $p < 0.001$  or ns: non-significance. ABE: adenine base editor, GFP: green fluorescent protein.

#### 14. Few RNA off-target effects were found after ABE treatments

We investigated ABE-mediated off-target RNA editing activities following each injected material. Adenine editing frequencies were measured using cDNA derived from four kinds of RNA transcripts (AARS1, PERP, TOPORS and MCM3AP). As a result of experiments using tissue samples from four regions, including frontal cortex, corpus callosum, heart and liver, both ABE8e and ABE8eWQ barely worked on non-targeted genomic sites. (Figure 27)

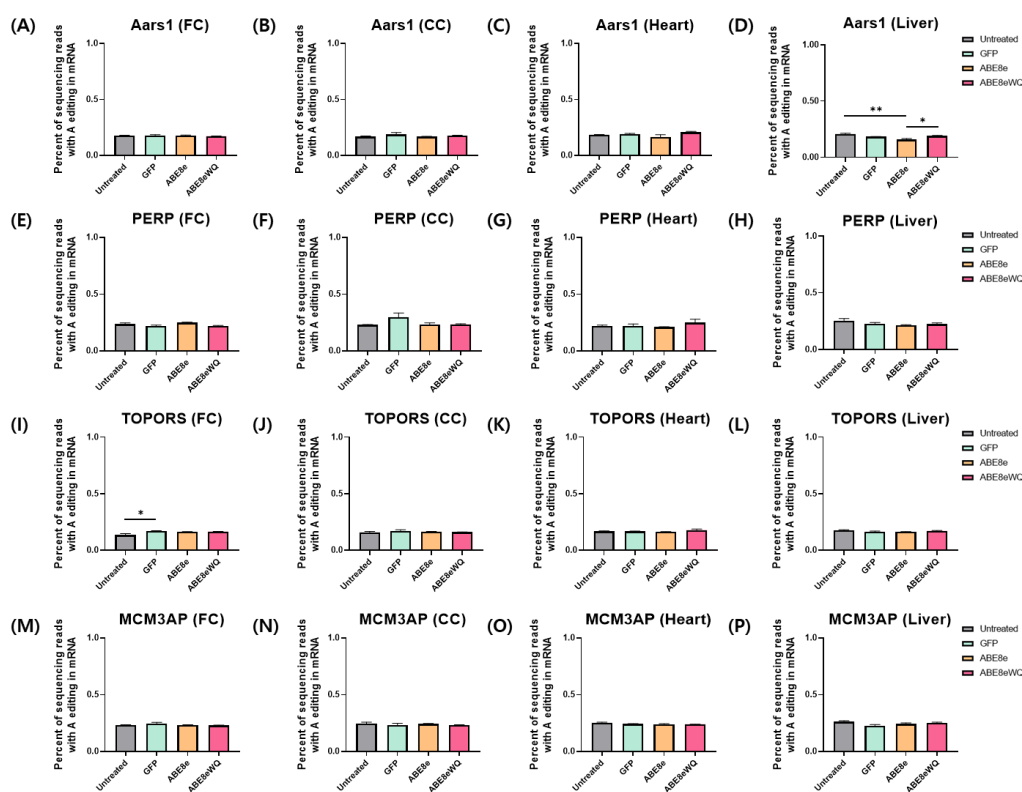


**Figure 27. Off-target RNA base editing in frontal cortex, corpus callosum, heart and liver.** Off-target effects in a few mouse organs after delivery of ABE8e and ABE8eWQ. Efficiencies of A-to-G mRNA editing are indicated. GFP treated mice and untreated mice were used as a control. (Untreated: n = 4, GFP: n = 4, ABE8e: n = 4, ABE8eWQ n = 4). Significant differences were rarely observed. Data were analyzed

using the one-way ANOVA and post-hoc comparisons (Bonferroni).  $*p < 0.05$ ,  $**p < 0.01$ ,  $***p < 0.001$ . The data are presented as mean  $\pm$  SEM. FC: frontal cortex, CC: corpus callosum, ABE: adenine base editor, AARS1: alanyl-tRNA synthetase 1, PERP: P53 apoptosis effector related to PMP22, TOPORS: topoisomerase I binding, arginine/serine-rich, MCM3AP: minichromosome maintenance complex component 3 associated protein.

#### IV. DISCUSSION

Base editing through ABE was successful in an *in vivo* experiment targeting mutated adenine on GALC gene in a Krabbe mouse model. Behavioral assessment on twitcher groups was conducted to confirm that the disease symptoms were significantly improved after ABE treatment. Additionally, behavioral assessment on young wild-type mouse groups and old wild-type mouse groups was conducted to confirm the safety of the ABE8e and ABE8eWQ. The levels of remyelination induced by ABE treatments in twitcher mouse were compared using techniques such as LFB/PAS, IF, EM, and MRI. These experimental results suggest that ABE8e and ABE8eWQ had an effect of alleviating the disease, but there was no significant difference between two of them.

In this study, main experiments focused on the difference between gene editing efficiency using ABE8e and ABE8eWQ. As result, whether using ABE8e or ABE8eWQ, any significant difference was not found in gene editing efficiency of target adenine. But gene editing effect on two non-target adenines as known as bystanders have significant difference between ABE8e and ABE8eWQ. ABE8e was more likely to correct wrong adenines compared to ABE8eWQ. When analyzing the degree of attachment to the off-target rather than the correct editing window, any significant difference was not found between ABE8e and ABE8eWQ. That is, the off-target effects of ABE8e and ABE8eWQ were similar.

The ICV injection which is an AAV delivery method we chose for current study had a limitation that the viral infection occurs almost exclusively in the brain. It means that it is difficult for being therapeutic materials to reach the peripheral nervous system. This may result in an inability to edit target adenine on GALC gene and restore the myelination of schwann cells surrounding peripheral nerves. These properties could be the reason why ABEs did not sufficiently prevent disease development and early death in twitcher.

Recent studies related to gene therapy have been reported various treatment approach to develop new injection methods and discover the optimal injection regions.<sup>11,12</sup> To find

the most efficient way to deliver ABE8e and ABE8eWQ, three additional studies can be suggested. First, a way to insert whole ABE gene into one viral vector should be devised. In this study, split ABE gene was used because whole ABE gene is too big to be packaged into one vector. So, if a new delivery vehicle such as virus like particle (VLP) that can accommodate the ABE gene at once is used, the ABE treatment effect can be enhanced. Second, attempts to treat ABEs by a different injection route should be made. Diverse AAV treatment methods have been developed such as intraperitoneal (IP), intravenous (IV), intramuscular (IM) and intrathecal (IT) injection, which enable the injected material better reaching peripheral nerves.<sup>20</sup> Last, combination therapy should be considered. This may be the most effective method to get adenine base editors to work most extensively and produce normal GALC enzymes which can restore the myelin of central nervous system and peripheral nervous system.

Moreover, gene therapy using adenine base editor can be applied to other various genetic diseases caused by G to A point mutation in addition to Krabbe disease. For example, there are beta-thalassemia which caused by G to A point mutation in human hemoglobin  $\beta$  (HBB) gene and porphyria which caused by a same type of mutation in hydroxymethylbilane synthase (HMBS) gene.<sup>21</sup>

## V. CONCLUSION

AAV gene therapy using two types of ABE is presented. To deliver adenine base editor named ABE8e and ABE8eWQ, AAV9 vectors were used during P1 intracerebroventricular (ICV) injection. Successful ICV injection of both ABE8e and ABE8eWQ improved neurobehavioral function and decreased both brain weight loss and body weight loss. Experiments are conducted to compare the two types of ABE on three criteria; editing efficiency, actual therapeutic effect and safety in a mouse model. As a result, there was a significant difference in the editing efficiency of two bystanders but no significant difference in therapeutic effect and side effect between ABE8e and ABE8eWQ treatment. Although the effect of ABE therapy in this study was weaker than that of traditional therapies, the most crucial thing is that the clinical application of adenine base editing is still a powerful candidate as complete treatment method for KD.

## REFERENCES

1. Suzuki, K., & Suzuki, K. (1995). The twitcher mouse: a model for Krabbe disease and for experimental therapies. *Brain pathology*, 5(3), 249-258.
2. Pan, X., Sands, S. A., Yue, Y., Zhang, K., LeVine, S. M., & Duan, D. (2019). An engineered galactosylceramidase construct improves AAV gene therapy for krabbe disease in twitcher mice. *Human Gene Therapy*, 30(9), 1039-1051.
3. Rafi, M. A., Rao, H. Z., Luzi, P., Curtis, M. T., & Wenger, D. A. (2012). Extended normal life after AAVrh10-mediated gene therapy in the mouse model of Krabbe disease. *Molecular Therapy*, 20(11), 2031-2042.
4. Li, Y., Miller, C. A., Shea, L. K., Jiang, X., Guzman, M. A., Chandler, R. J., et al. (2021). Enhanced efficacy and increased long-term toxicity of CNS-directed, AAV-based combination therapy for Krabbe disease. *Molecular Therapy*, 29(2), 691-701.
5. Mikulka, C. R., & Sands, M. S. (2016). Treatment for Krabbe's disease: Finding the combination. *Journal of neuroscience research*, 94(11), 1126-1137.
6. Hess, G. T., Tycko, J., Yao, D., & Bassik, M. C. (2017). Methods and applications of CRISPR-mediated base editing in eukaryotic genomes. *Molecular cell*, 68(1), 26-43.
7. Koblan, L.W., Doman, J.L., Wilson, C., Levy, J.M., Tay, T., Newby, G.A., et al. (2018). Improving cytidine and adenine base editors by expression optimization and ancestral reconstruction. *Nat Biotechnol* 36, 843-846. 10.1038/nbt.4172.
8. Levy, J.M., Yeh, W.H., Pendse, N., Davis, J.R., Hennessey, E., Butcher, R., et al. (2020). Cytosine and adenine base editing of the brain, liver, retina, heart and skeletal muscle of mice via adeno-associated viruses. *Nat Biomed Eng* 4, 97-110. 10.1038/s41551-019-0501-5.
9. Ryu, S.M., Koo, T., Kim, K., Lim, K., Baek, G., Kim, S.T., et al. (2018). Adenine base editing in mouse embryos and an adult mouse model of Duchenne muscular dystrophy. *Nat Biotechnol* 36, 536-539. 10.1038/nbt.4148.

10. Song, C.Q., Jiang, T., Richter, M., Rhym, L.H., Koblan, L.W., Zafra, M.P., et al. (2020). Adenine base editing in an adult mouse model of tyrosinaemia. *Nat Biomed Eng* 4, 125-130. 10.1038/s41551-019-0357-8.
11. Rees, H. A., & Liu, D. R. (2018). Base editing: precision chemistry on the genome and transcriptome of living cells. *Nature reviews genetics*, 19(12), 770-788.
12. Song, C. Q., Jiang, T., Richter, M., Rhym, L. H., Koblan, L. W., Zafra, M. P., et al. (2020). Adenine base editing in an adult mouse model of tyrosinaemia. *Nature Biomedical Engineering*, 4(1), 125-130.
13. Hordeaux, J., Jeffrey, B. A., Jian, J., Choudhury, G. R., Michalson, K., Mitchell, T. W., et al. (2022). Efficacy and safety of a Krabbe disease gene therapy. *Human Gene Therapy*, 33(9-10), 499-517.
14. Cantuti-Castelvetri, L., Maravilla, E., Marshall, M., Tamayo, T., D'Auria, L., Monge, J., et al. (2015). Mechanism of neuromuscular dysfunction in Krabbe disease. *J Neurosci* 35, 1606-1616. 10.1523/JNEUROSCI.2431-14.2015.
15. De Gasperi, R., Friedrich, V.L., Perez, G.M., Senturk, E., Wen, P.H., Kelley, K., et al. (2004). Transgenic rescue of Krabbe disease in the twitcher mouse. *Gene Ther* 11, 1188-1194. 10.1038/sj.gt.3302282.
16. Deber CM, Reynolds SJ (April 1991). Central nervous system myelin: structure, function, and pathology. *Clinical Biochemistry*. 24 (2): 113–134. 10.1016/0009-9120(91)90421-a
17. Saxe DF, Takahashi N, Hood L, Simon MI (1985). Localization of the human myelin basic protein gene (MBP) to region 18q22----qter by in situ hybridization. *Cytogenetics and Cell Genetics*. 39 (4): 246–249. 10.1159/000132152
18. Boggs JM (September 2006). "Myelin basic protein: a multifunctional protein". *Cellular and Molecular Life Sciences*. 63 (17): 1945–1961. 10.1007/s00018-006-6094-7
19. Inamura, N., Kito, M., Go, S., Kishi, S., Hosokawa, M., Asai, K., et al. (2018). Developmental defects and aberrant accumulation of endogenous psychosine in

- oligodendrocytes in a murine model of Krabbe disease. *Neurobiol Dis* 120, 51-62.  
10.1016/j.nbd.2018.08.023.
20. Heller, G. J., Marshall, M. S., Issa, Y., Marshall, J. N., Nguyen, D., Rue, E., et al. (2021). Waning efficacy in a long-term AAV-mediated gene therapy study in the murine model of Krabbe disease. *Molecular Therapy*, 29(5), 1883-1902.
21. Félix, A. J., Solé, A., Noé, V., & Ciudad, C. J. (2020). Gene Correction of Point Mutations Using PolyPurine Reverse Hoogsteen Hairpins Technology. *Frontiers in Genome Editing*, 2, 583577.

ABSTRACT(IN KOREAN)

크라베병 마우스 모델을 활용한  
ABE8e와 ABE8eWQ의 유전자 편집 효율 비교

<지도교수 조성래>

연세대학교 대학원 의과학과

김주희

크라베 병은 상염색체 열성으로 유전되는 질환으로 지질 분해에 필요한 효소 GALC가 결핍되어 발생한다. 이 병은 중추신경계와 말초신경계를 함께 침범하는 백질이영양증을 일으킨다. 현재까지 많은 연구자들은 GALC 효소를 주입하여 이 질환을 완화하기 위한 치료제를 개발해 왔지만, 우리는 점 돌연변이로 인해 발생하는 이 질환을 아데닌 염기 교정법을 사용해 유전자 수준에서 병인을 제거하는 방향으로 치료하고자 한다. 이 연구에서는 ABE8e와 ABE8eWQ라는 두 종류의 ABE의 타겟 유전자 교정 효율뿐만 아니라 비특이적이고 의도하지 않은 유전자 변형 발생 수준까지 비교했다. 이것이 치료제의 안전성과 직결된다고 여겼기 때문이다. ABE8eWQ는 ABE8e를 기반으로 비표적 변이 효과는 감소하고 표적 아데닌의 교정 효과는 증가된 표적 특이적 유전자 가위를 만들기 위해 개발되었다. 따라서 마우스 모델의 체내에서 더 적은 부작용을 나타낼 것으로 사료되었다.

실제로 bystander non-target adenine의 교정율은 ABE8eWQ에서 유의하게 낮았다. 그러나 두 종류의 ABE 주입 질병군에서 모두 체중 및 수명이 증가하고, 떨림 현상이 감소하고, 행동 평가 고득점을 기록했다. 조직학적 분석을 통해서도 ABE 주입 후 미엘린 수초의 회복이 관찰되었다. 결론적으로, 두 종류의 ABE 모두 전반적인 질병 증상 완화에 도움을 주었다는 것이다.

---

핵심되는 말 : 크라베병, 신경퇴행성질환, 유전자 편집, 아데닌 염기 교정법, 아데노 연관 바이러스, 탈수초화

#### PUBLICATION LIST

1. Pyo, S., Kim, J., Hwang, J., Heo, J. H., Kim, K., Cho, S. R. (2022). Environmental Enrichment and Estrogen Upregulate Beta-Hydroxybutyrate Underlying Functional Improvement. *Frontiers in Molecular Neuroscience*, 15.